Inertial Navigation Systems

Kiril Alexiev

Navigation

Estimate the position and orientation.

Inertial navigation – one of possible instruments.
Newton law is used:

$$F = am$$

Acceleration and angular velocity are measured.

Inertial Sensors

Most common inertial sensors:
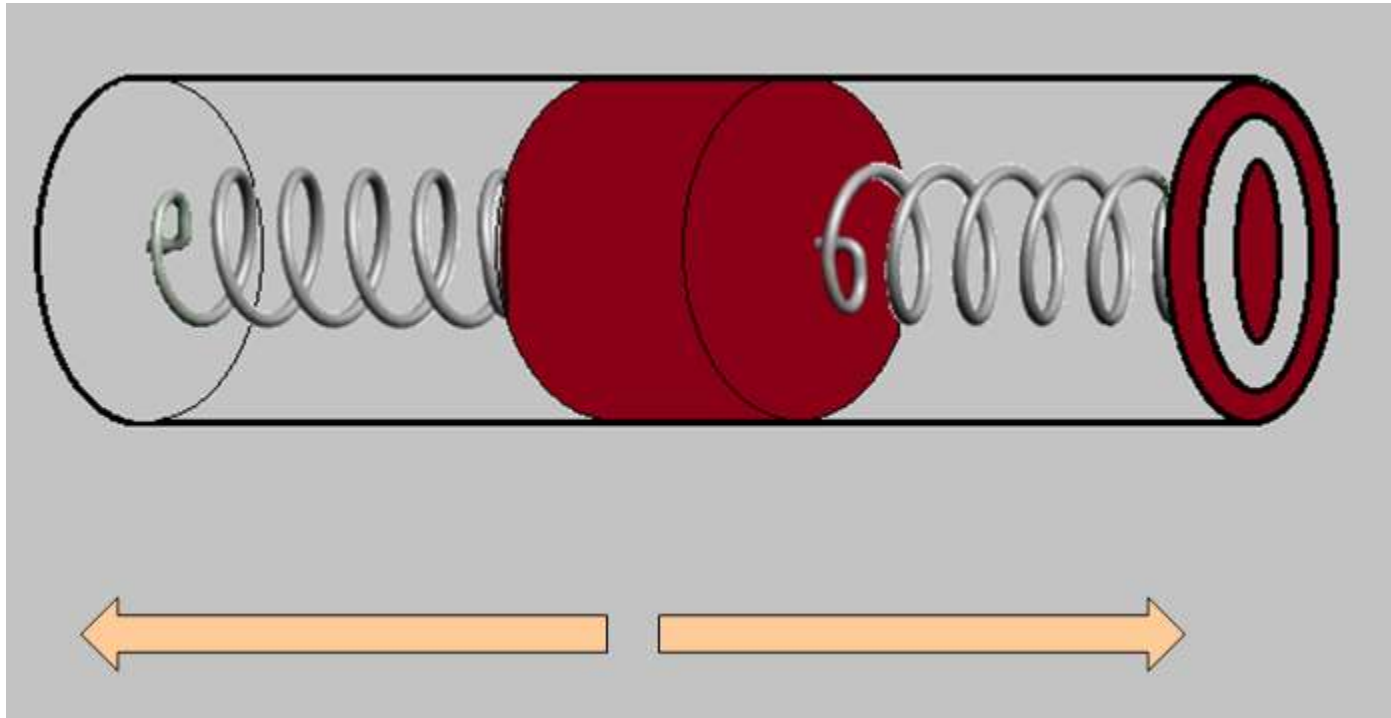
• *Accelerometers*

    The accelerometers detect the combined magnitude and direction of linear and *gravitational* *accelerations*
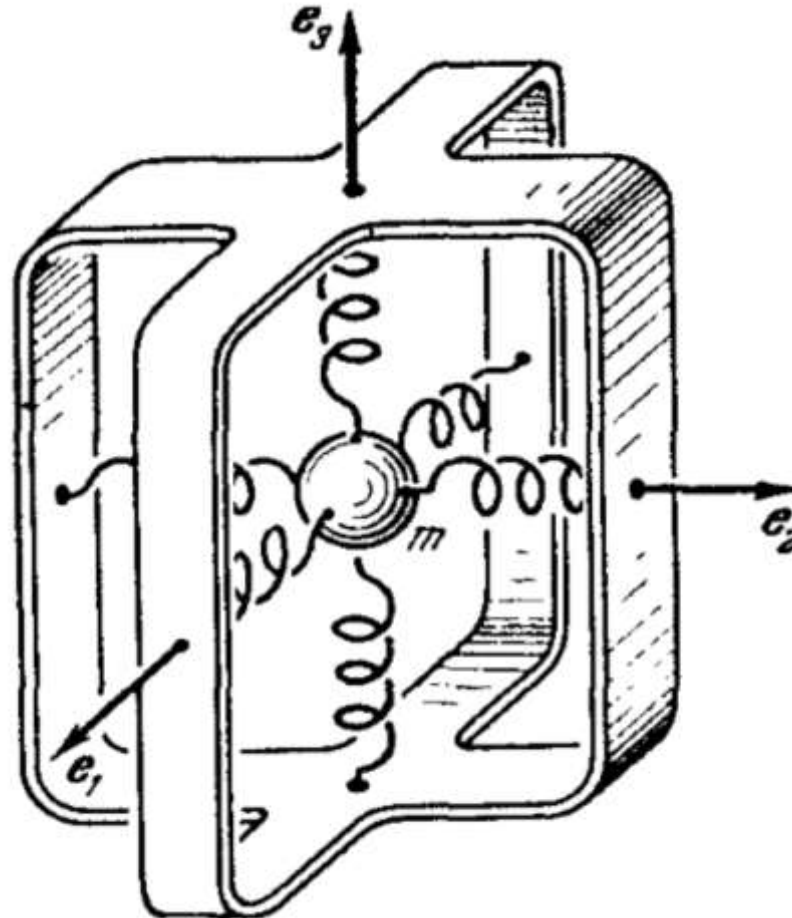
• *Gyros*

    The gyroscopes measure the angular rate of rotation about one or more axes. They are not dependent on gravity.
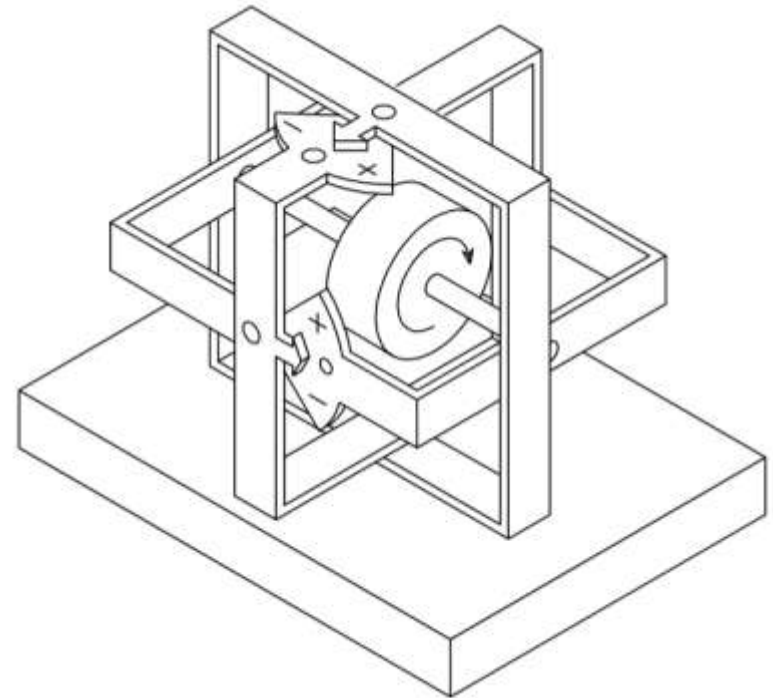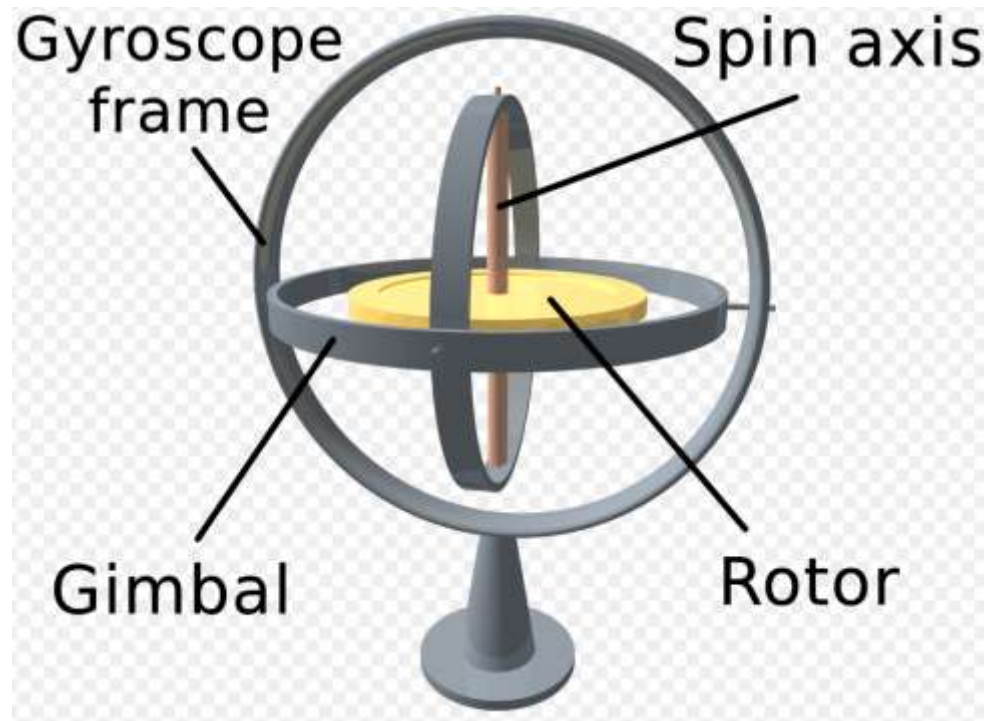
Accelerometers

Proof mass and two springs, g will be also measured
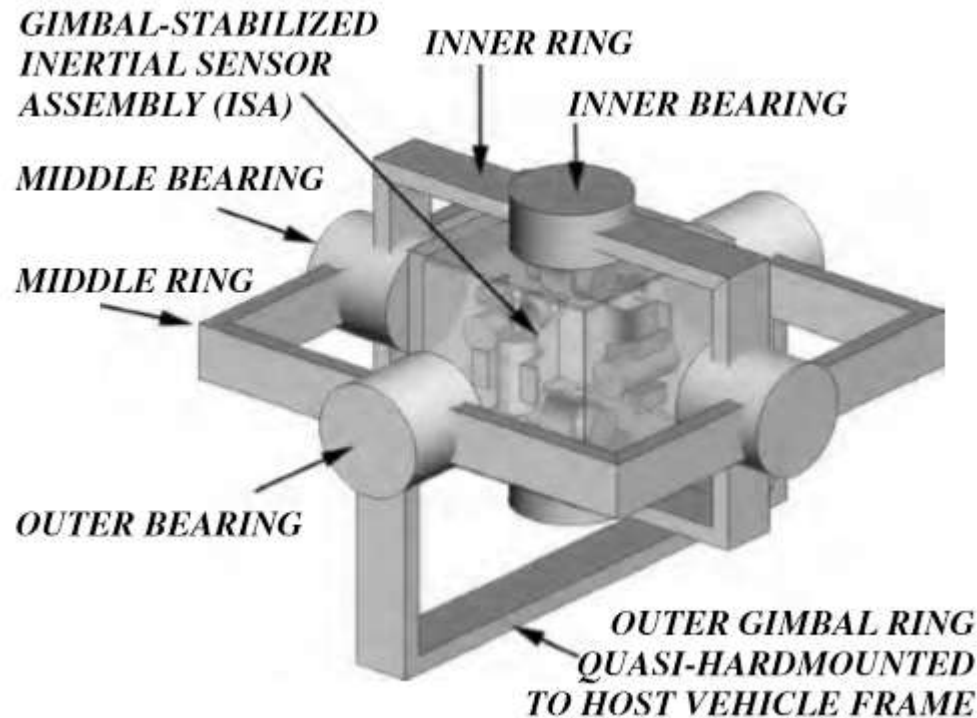
3D Accelerometers

Gyroscope

Gyroscope measures the angles of rotation according initial position

Gyrostabilazed platform with accelerometers

GIMBAL-STABILIZED
INERTIAL SENSOR
ASSEMBLY (ISA)

INNER RING

INNER BEARING

MIDDLE BEARING

MIDDLE RING

OUTER BEARING

OUTER GIMBAL RING
QUASI-HARDMOUNTED
TO HOST VEHICLE FRAME

Accelerometers measure acceleration in a fixed coordinate system. These INS are called gimbaled system.
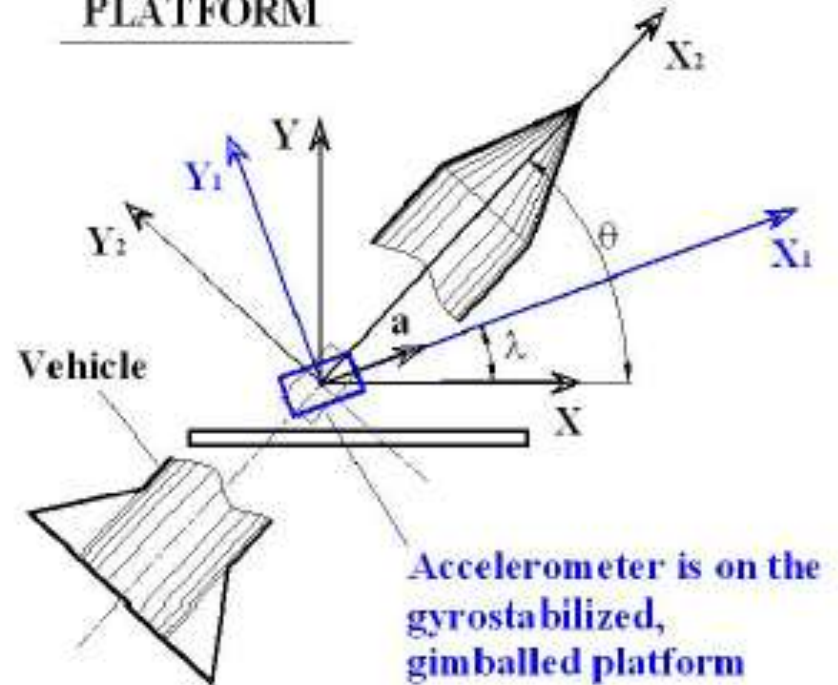
Strapdown INS

In late sixties there was proved that gimbals could be modeled mathematically and gimbals could not be used. Such kind of INS were called strapdown, because the inertial sensors are fixed on the body of moving object. Technical advanced in electronics reduced the size and cost of inertial sensors. They became MEMS. Lower cost and higher reliability supported replacement of mechanisms in classical understanding with electronics.

Types of INS

STRAPDOWN

Accelerometer is strapdown to the vehicles body

PLATFORM
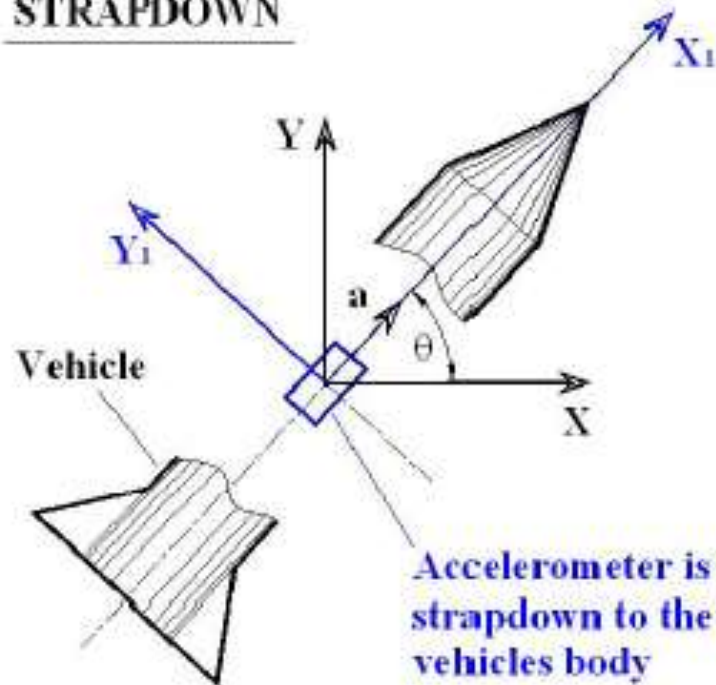
Accelerometer is on the gyrostabilized, gimballed platform

Strapdown ⬅➡Gimbailed

The inertial sensors of a strapdown system fully follow the vehicle's angular motion. Hence, the measurement of specific force must be transformed from the body frame into that reference coordinate frame in which the integrations of acceleration are to take place.

In gimbailed navigation systems, the inertial sensors are mounted on gimbals whose orientations are nominally stationary relative to either the intermediate or the reference coordinate frame.

The performance of a strapdown system is limited primarily by two factors not present in gimballed navigation systems. In gimbailed navigation systems, the inertial sensors are mounted on gimbals whose orientations are nominally stationary relative to either the intermediate or the reference coordinate frame. The inertial sensors of a strapdown system fully follow the vehicle's angular motion. Hence, the measurement of specific force must be transformed from the body frame into that reference coordinate frame in which the integrations of acceleration are to take place.

Each small rotation increment represents a finite rotation. However, finite rotations do not commute, since Rotation A followed by Rotation B does not, in general, produce the same result as Rotation B followed by Rotation A. Consequently, coordinate transformations computed from these finite increments include, to some degree, errors resulting from the noncommutativity of finite rotations. The size of these errors depends upon the size of the increment and upon the sophistication of the algorithm used in updating the coordinate transformation.

Why MEMS?

These sensors are inexpensive: most MEMS sensors in mass production quantities cost a few dollars. These sensors are truly miniature - usually less than (10x10x5 mm) in size, and they consume little power (< 50 mA).

Why not MEMS?

The biases of MEMS gyros can be brought down to a level of less than 300 degrees per hour after appropriate temperature compensation. Such a large drift, even assuming an accurate initialization of attitude, will lead to very large position errors after almost 10 seconds of INS-only navigation.

Part #	Gyro Full Scale Range	Gyro Sensitivity	Gyro Rate Noise	Accel Full Scale Range	Accel Sensitivity	Digital Output	Logic Supply Voltage	Operating Voltage Supply	Package Size
UNITS:	(°/sec)	(LSB/°/sec)	(dps/√Hz)	(g)	(LSB/g)		(V)	(V +/-5%)	(mm)
MPU-6000	±250 ±500 ±1000 ±2000	131 65.5 32.8 16.4	0.005	±2 ±4 ±8 ±16	16384 8192 4096 2048	I²C or SPI	VDD	2.375V–3.46V	4x4x0.9
MPU-6050	±250 ±500 ±1000 ±2000	131 65.5 32.8 16.4	0.005	±2 ±4 ±8 ±16	16384 8192 4096 2048	I²C	1.8V±5% or VDD	2.375V–3.46V	4x4x0.9

GYROSCOPE SENSITIVITY					
Full-Scale Range	FS_SEL=0		±250		°/s
	FS_SEL=1		±500		°/s
	FS_SEL=2		±1000		°/s
	FS_SEL=3		±2000		°/s
Gyroscope ADC Word Length			16		bits
Sensitivity Scale Factor	FS_SEL=0		131		LSB/(°/s)
	FS_SEL=1		65.5		LSB/(°/s)
	FS_SEL=2		32.8		LSB/(°/s)
	FS_SEL=3		16.4		LSB/(°/s)
Sensitivity Scale Factor Tolerance	25°C	-3		+3	%
Sensitivity Scale Factor Variation Over Temperature			±2		%
Nonlinearity	Best fit straight line; 25°C		0.2		%
Cross-Axis Sensitivity			±2		%
GYROSCOPE NOISE PERFORMANCE	**FS_SEL=0**				
Total RMS Noise	DLPFCFG=2 (100Hz)		0.05		°/s-rms
Low-frequency RMS noise	Bandwidth 1Hz to10Hz		0.033		°/s-rms
Rate Noise Spectral Density	At 10Hz		0.005		°/s/ √ Hz
GYROSCOPE MECHANICAL FREQUENCIES					
X-Axis		30	33	36	kHz
Y-Axis		27	30	33	kHz
Z-Axis		24	27	30	kHz
LOW PASS FILTER RESPONSE					
	Programmable Range	5		256	Hz

ACCELEROMETER SENSITIVITY				
Full-Scale Range	AFS_SEL=0	±2		*g*
	AFS_SEL=1	±4		*g*
	AFS_SEL=2	±8		*g*
	AFS_SEL=3	±16		*g*
ADC Word Length	Output in two's complement format	16		bits
Sensitivity Scale Factor	AFS_SEL=0	16,384		LSB/*g*
	AFS_SEL=1	8,192		LSB/*g*
	AFS_SEL=2	4,096		LSB/*g*
	AFS_SEL=3	2,048		LSB/*g*
Initial Calibration Tolerance		±3		%
Sensitivity Change vs. Temperature	AFS_SEL=0, -40°C to +85°C	±0.02		%/°C
Nonlinearity	Best Fit Straight Line	0.5		%
Cross-Axis Sensitivity		±2		%

ZERO-G OUTPUT				
Initial Calibration Tolerance[1]	X and Y axes	±50		mg
	Z axis	±80		mg
Zero-G Level Change vs. Temperature	X and Y axes, 0°C to +70°C	±35		
	Z axis, 0°C to +70°C	±60		mg
SELF TEST RESPONSE				
		300	950	mg
NOISE PERFORMANCE				
Power Spectral Density	@10Hz, AFS_SEL=0 & ODR=1kHz	400		µg/ √ Hz

TABLE I.   ACCUMULATED ERROR DUE TO ACCELEROMETER BIAS ERROR

Grade	Accel. Bias Error [mg]	Horizontal Position Error [m]			
		1 s	10 s	60 s	1 hr
Navigation	0.025	0.00013	0.012	0.44	1600
Tactical	0.3	0.0015	0.15	5.3	19000
Industrial	3	0.015	1.5	53	190000
Automotive	125	0.62	60	2200	7900000

TABLE II.   ACCUMULATED ERROR DUE TO ACCELEROMETER MISALIGNMENT

Accelerometer Misalignment [deg]	Horizontal Position Error [m]			
	1 s	10 s	60 s	1 hr
0.050	0.0043	0.43	15	57000
0.10	0.0086	0.86	31	110000
0.50	0.043	4.3	150	570000
10	0.086	8.6	310	1100000

TABLE III. ACCUMULATED ERROR DUE TO GYRO ANGLE RANDOM WALK

Grade	Gyro Angle Random Walk [deg/√hr]	Horizontal Position Error [m]			
		1 s	10 s	60 s	1 hr
Navigation	0.002	0.00001	0.0001	0.0013	620
Tactical	0.07	0.0001	0.0032	0.046	22000
Industrial	3	0.01	0.23	3.3	1500000
Automotive	5	0.02	0.45	6.6	3100000

TYPICAL PERFORMANCE CHARACTERISTICS
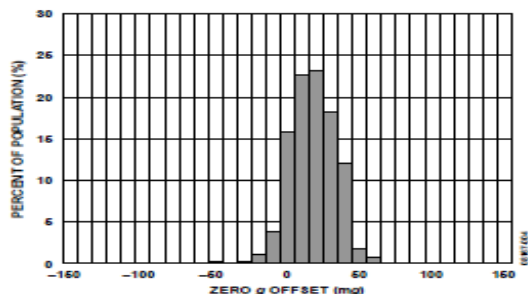
Figure 4. X-Axis Zero g Offset at 25°C, $V_S = 2.6$ V
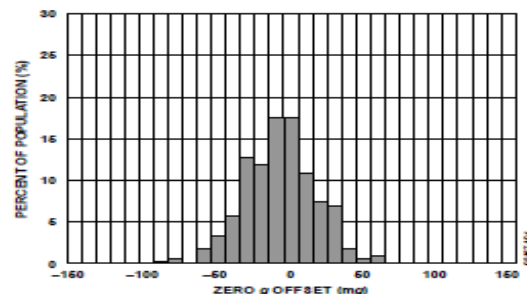
Figure 7. X-Axis Zero g Offset at 25°C, $V_S = 1.8$ V
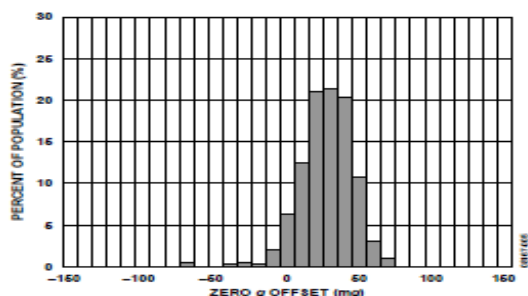
Figure 5. Y-Axis Zero g Offset at 25°C, $V_S = 2.6$ V
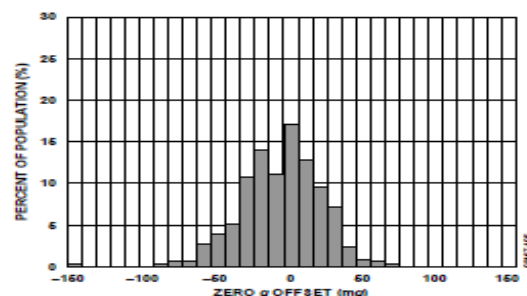
Figure 8. Y-Axis Zero g Offset at 25°C, $V_S = 1.8$ V
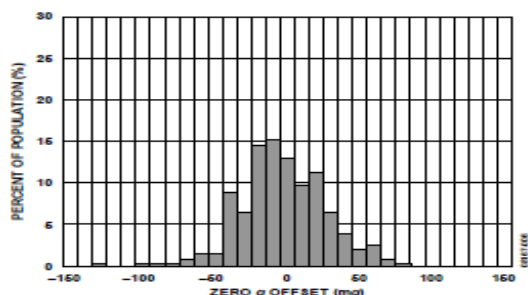
Figure 6. Z-Axis Zero g Offset at 25°C, $V_S = 2.6$ V
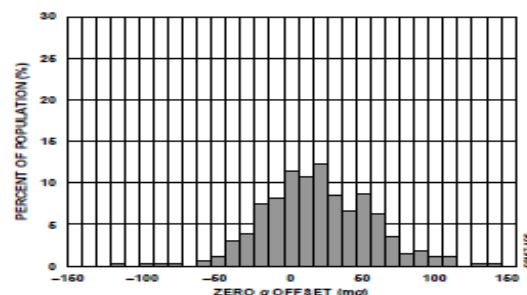
Figure 9. Z-Axis Zero g Offset at 25°C, $V_S = 1.8$ V

The Coriolis-effect

Let assume a mass that is vibrating in the radial direction of a rotating system. Due to the Coriolis force working perpendicular to the original vibrating direction, a new vibration will take place in this direction. The amplitude of this new vibration is a function of the angular velocity. MEMS gyros (MicroElectroMechanical Systems), "tuning fork"and "wineglass"gyros are utilizing this principle. Coriolis-based gyros are typically cheaper and less accuratethan mechanical, ring laser or fiber optic gyros.
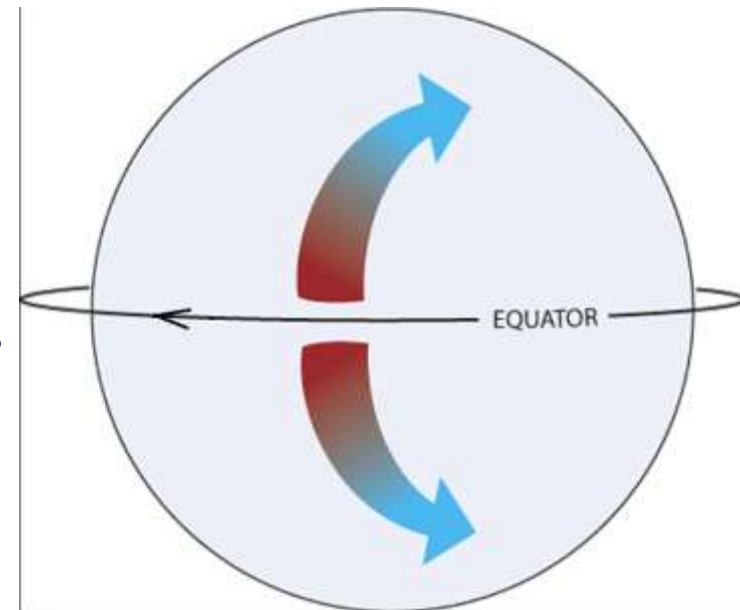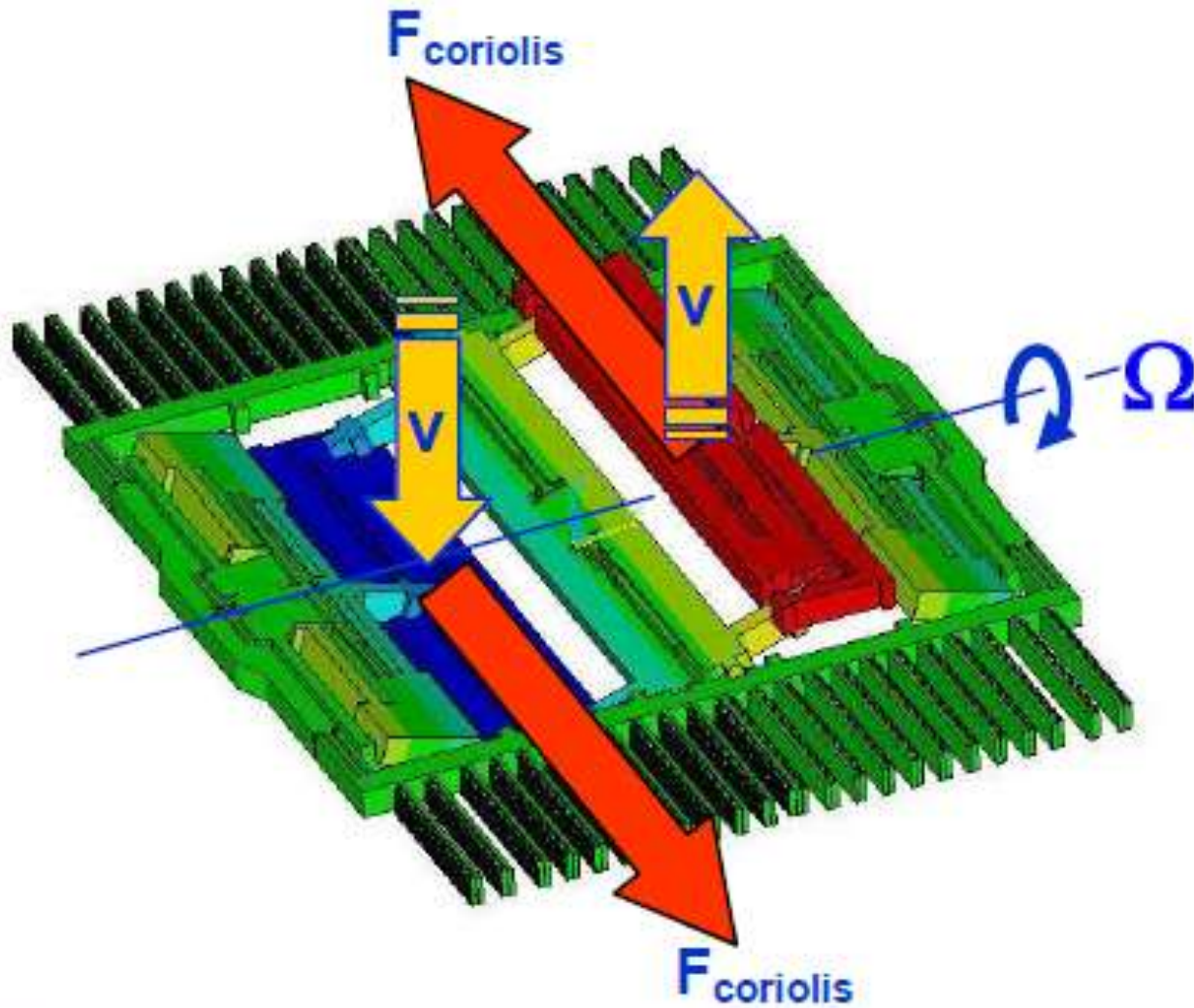
Figure 3: X-axis gyroscope driven mode
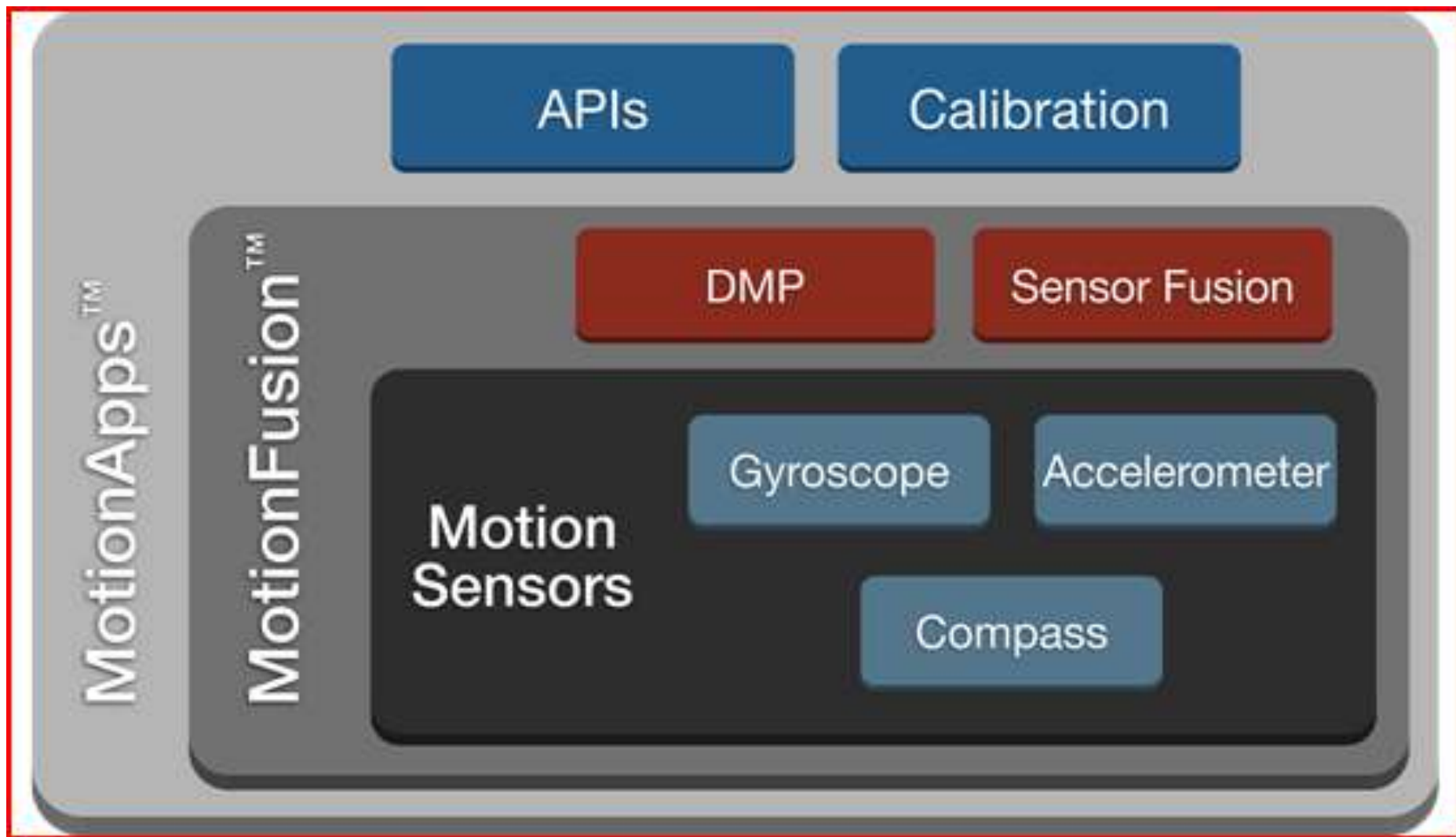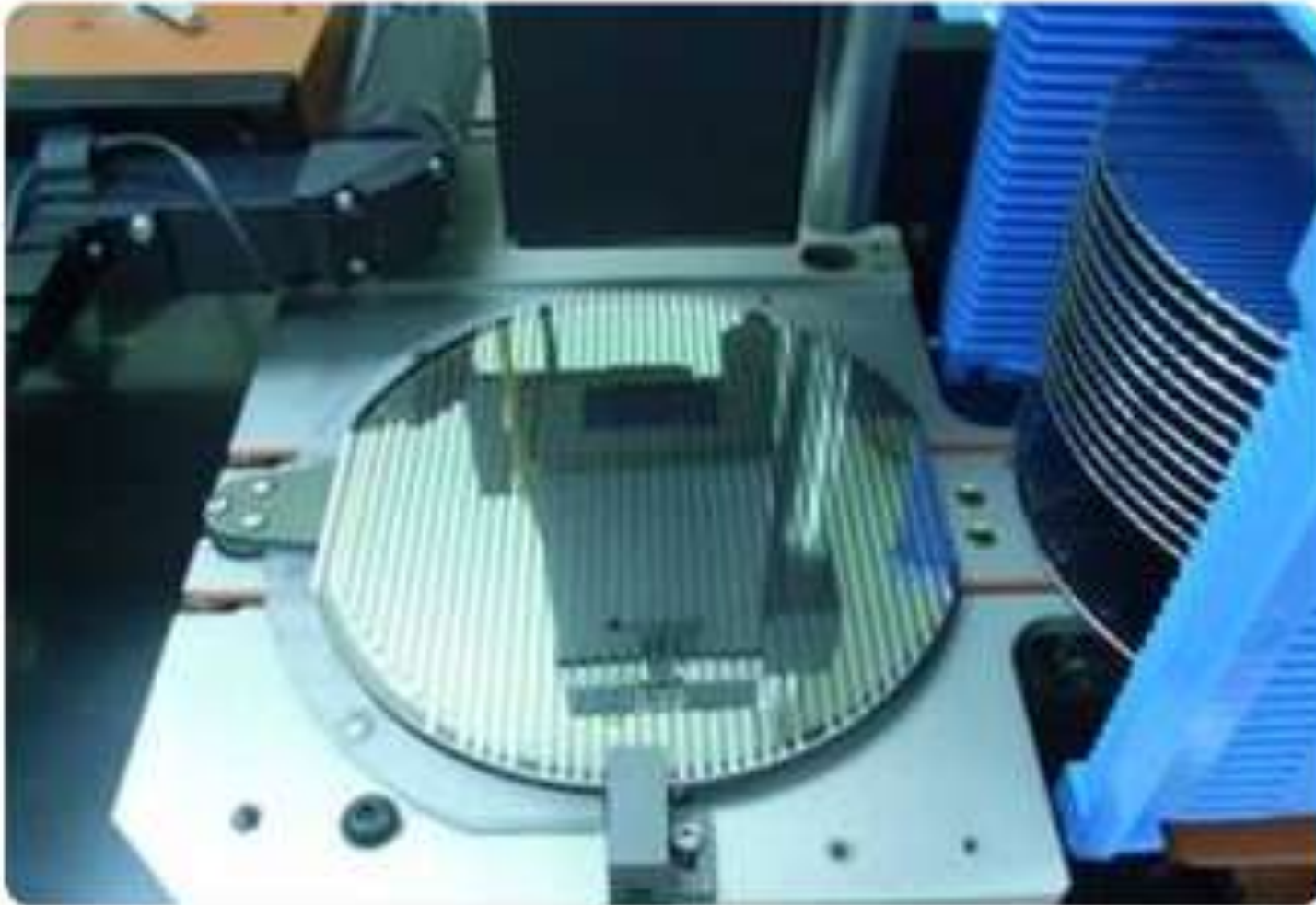
MEMS Manufacturing Process

MPU-9150 Motion Tracking device

MPU-6050

Figure 1. Top side of the MPU-60X0 9-Axis EV Board
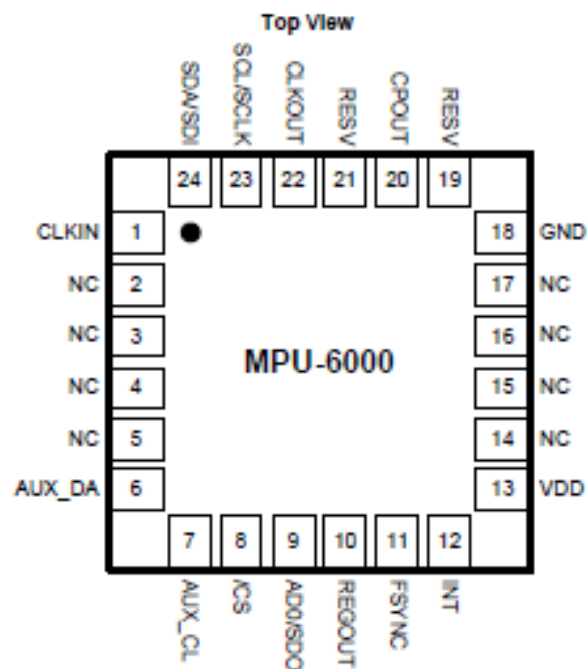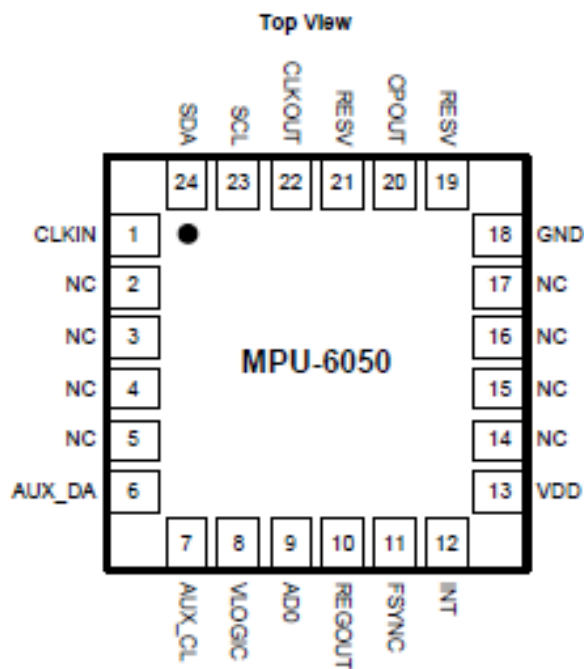
Figure 2. MPU-6000 QFN Package (Top View) 24-pin 4mm x 4mm x 0.9mm & Axis Orientation

(a) The engineered silicon on insulator (ESOI) wafer is formed starting with a standard silicon handle wafer etched with simple targets for backside alignment (mask 1); followed by oxidation and cavity etch (mask 2). A second wafer is fusion bonded to the handle wafer and subsequently thinned to define the device layer thickness.

(b) The MEMS wafer is completed by etching the device layer to form standoffs (mask 3) that define the seal ring, the electrical contacts to CMOS, and the vertical gap between the CMOS and MEMS; depositing and patterning a germanium layer (mask 4) over standoffs; and patterning (mask 5) and deep reactive ion etching the device layer to form the mechanical structure.

(c) A standard CMOS wafer is fabricated by an independent foundry, and cavities (mask 6) can be etched into the CMOS wafer, if needed for larger clearance under moving MEMS structures.

(d) The MEMS wafer is bonded to the CMOS wafer using AlGe eutectic bonding between the Al on the CMOS and the Ge on the MEMS wafer. After bonding, a portion of the MEMS wafer is removed by conventional dicing saw cuts to expose the CMOS wire bond pads.
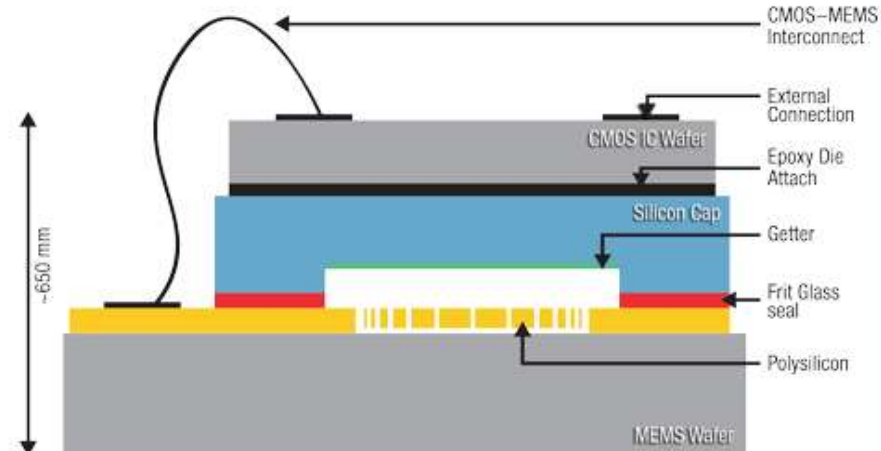
Figure 1: Simple six mask Nasiri-Fabrication process flow.

Nasiri Fabrication Platform
CMOS-MEMS Structure
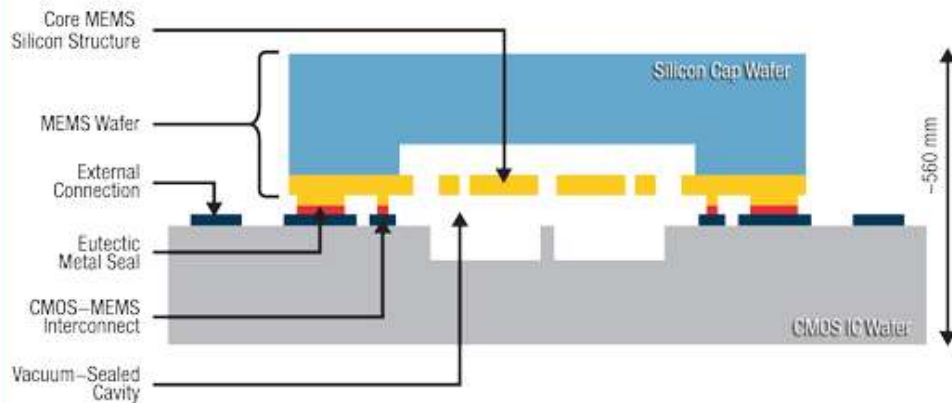
Traditional MEMS Fabrication
MEMS SIP Packaging

Comparison of Fabrication Platforms
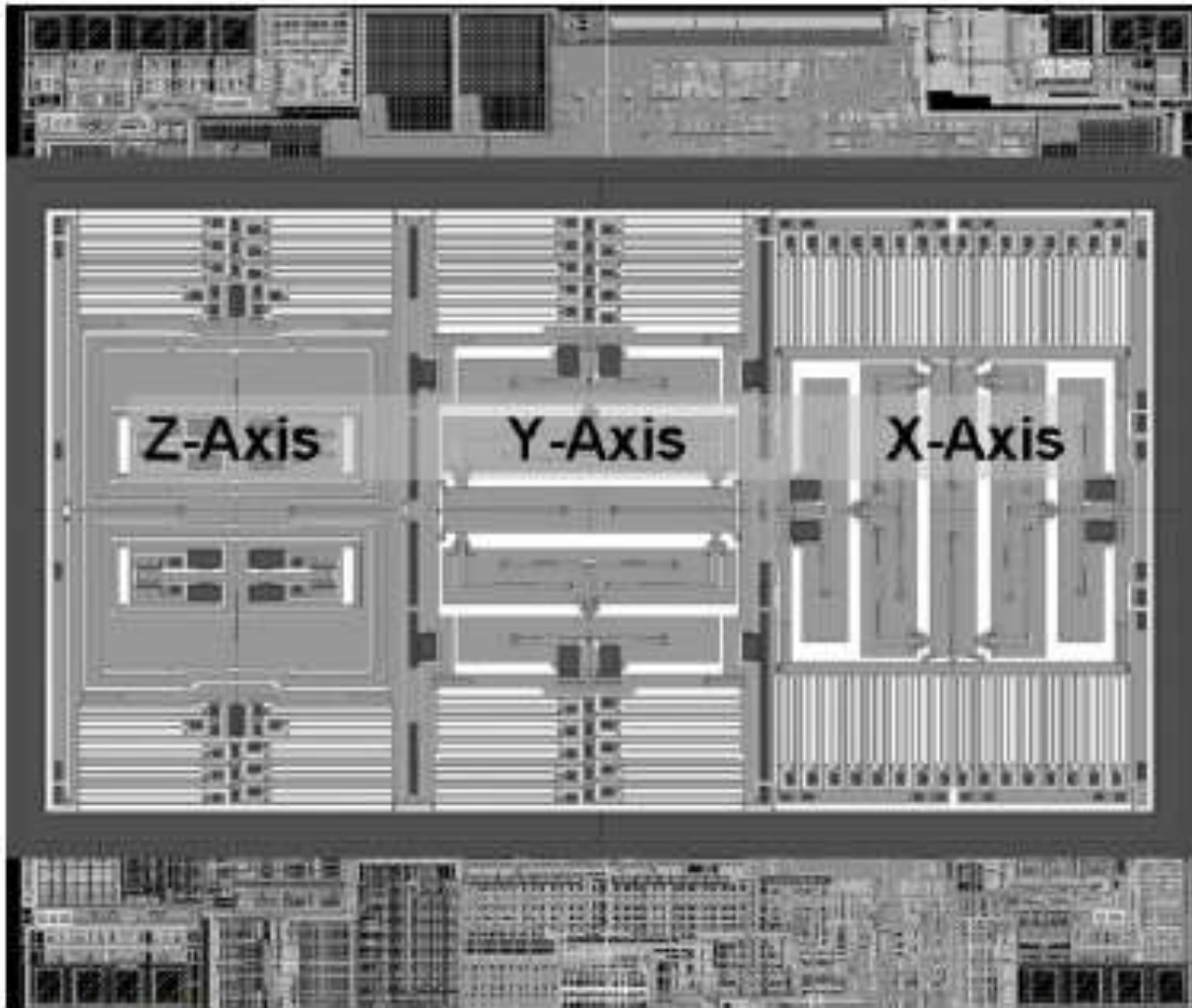
Figure 7: MPU-3000, 3-Axis gyroscope in 2.8mm x 2.4mm

Optical gyros

The Sagnac-effect.The inertial characteristics of lightcan also be utilized, by letting two beams of light travel in a loop in opposite directions. If the loop rotates clockwise, the clockwise beam must travel a longer distance before finishing the loop. The opposite is true for the counter-clockwise beam. Combining the two rays in a detector, an interference patternis formed, which will depend on the angular velocity.

RING LASER GYROS

- *An electronic processor calculates the difference between the frequencies of the two laser beams.*

- *The rate of rotation of the gyro determines the phase difference of the frequencies. Each particular phase difference coincides with a unique rate of turn which the processor can thus calculate.*

- *Each ring laser gyroscope only rotates on one axis, therefore three of them are required to register changes in pitch, roll, and yaw.*

ADVANTAGES

- *Few moving parts*
- *Small size and light weight*
- *Rigid construction*
- *High tolerance to shock, acceleration, and vibration*
- *High level of accuracy*
- *Low cost over the lifetime of the gyro*
- *Because there are no rotating gimbals as in a mechanical gyro, there is no friction, and therefore no errors caused by real precession*
- *Less power consumed than mechanical gyros because there are fewer moving parts.*

DISADVANTAGES

- *Base cost of Laser ring gyros is more expensive than mechanical gyros.*
- *Laser ring gyros are susceptible to an error known as "LOCK-IN"*

LOCK-IN

When the rate of turn is very small, the frequency difference between the two beams is small.
There is a tendency for the two frequencies to "couple" together and "lock-in" with each other.
As a result of lock-in, a zero turning rate is indicated.
While lock-in errors are not substantial, they can be accounted for by using more complex ring laser gyro systems.
By mechanically moving or twisting the system, the coupling of frequencies does not occur.
This mechanical adjustment is called DITHERING.

Figure 4. Types of laser gyros

Active

Passive
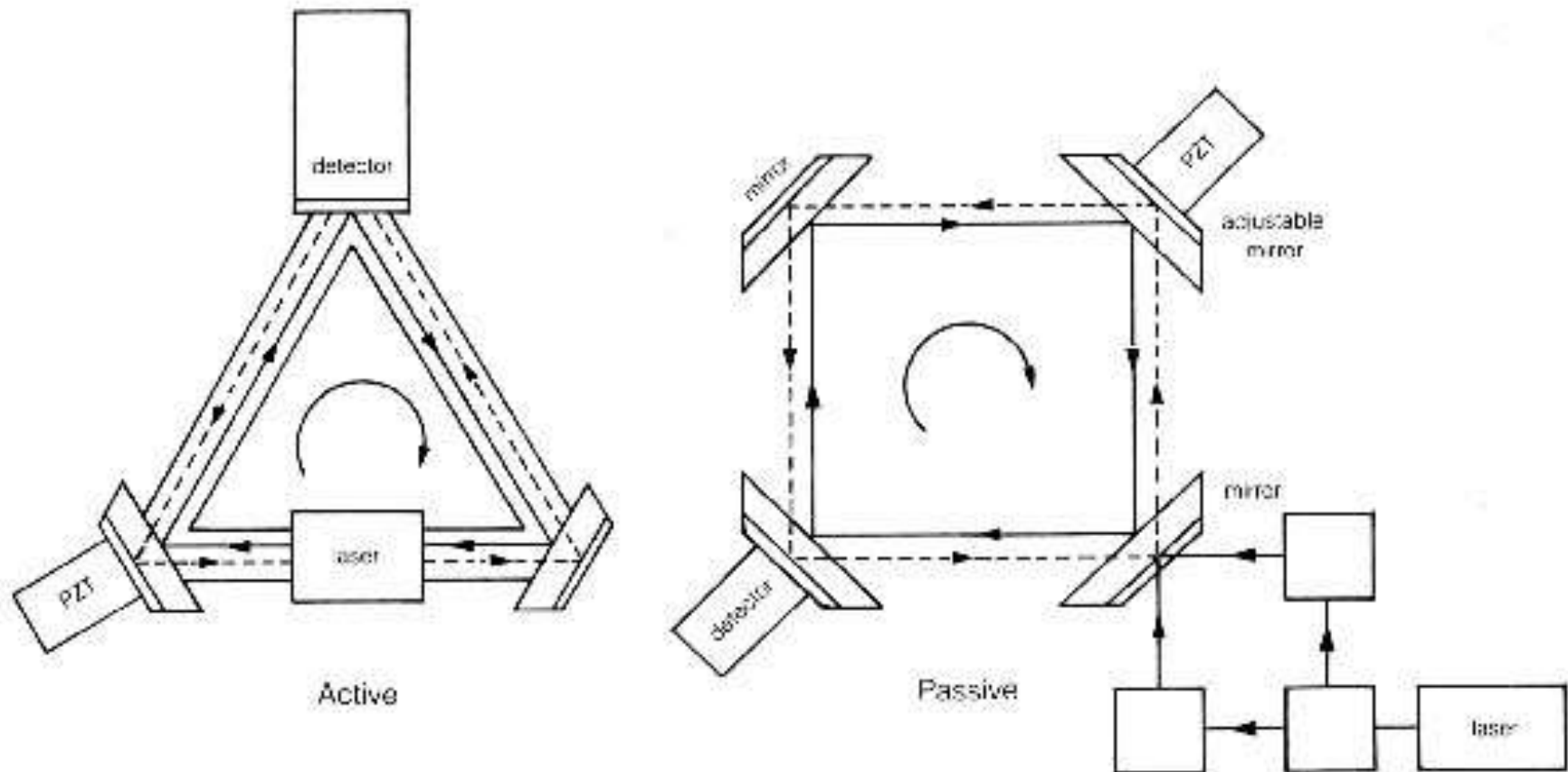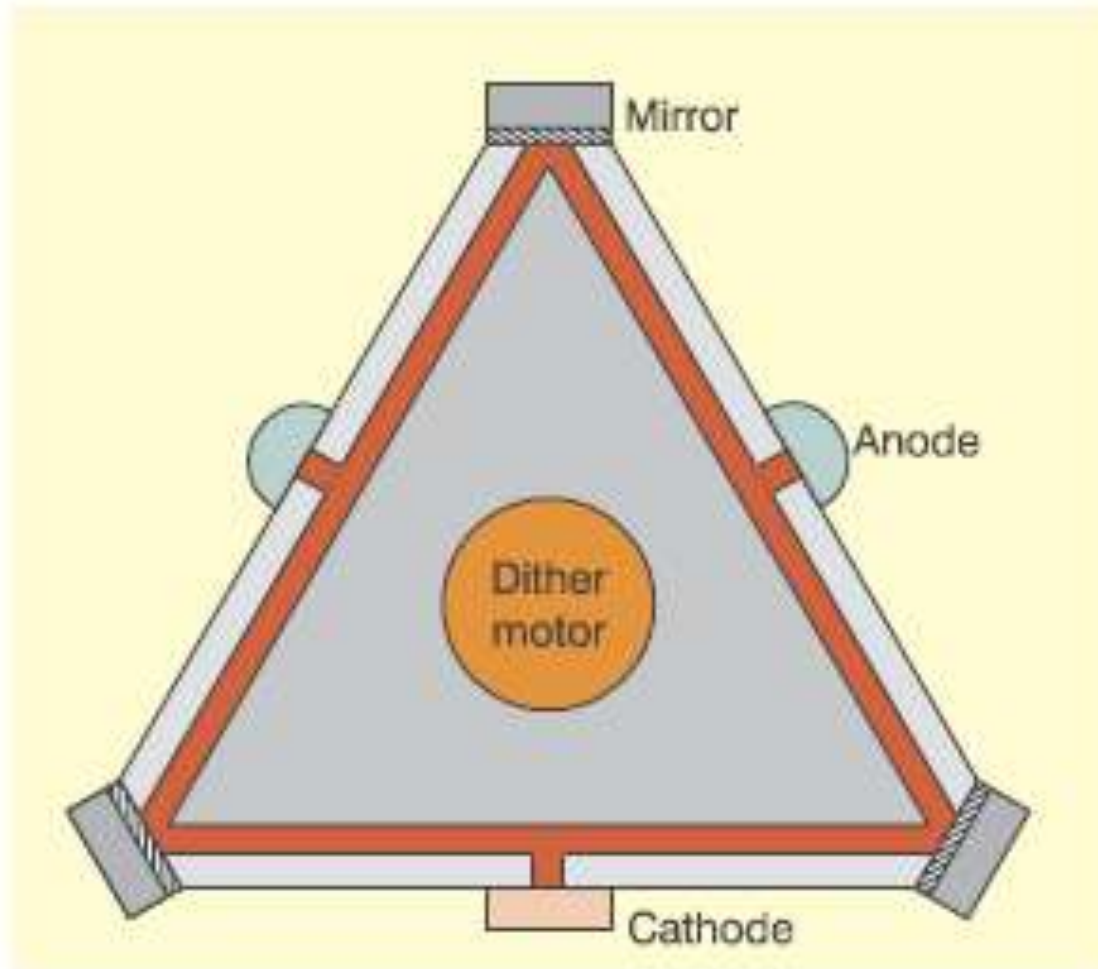
lamp). The discharge provides enough energy to   amounts of backscatter, which couples energy
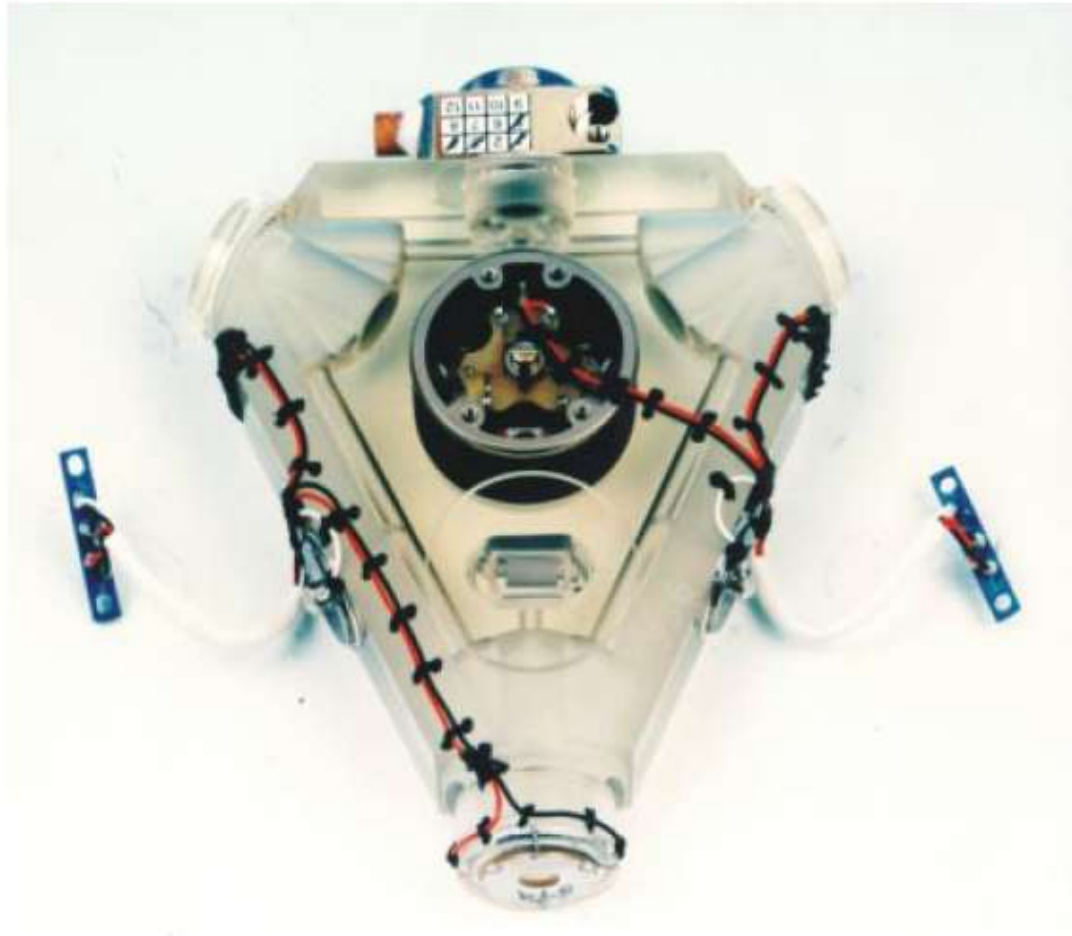
9.   *Photograph of a ring laser gyro.*

IMU

Several inertial sensors are often assembled to form an Inertial Measurement Unit (IMU).

Typically the unit has 3 accelerometers and 3 gyros (x, y and z), often 3 magnitometers (compass).

Example (Strapdown IMU)

Honeywell HG1700 ("medium quality"): 3 accelerometers, accuracy: 1 mg, 3 ring laser gyros, accuracy: 1 deg/h, Rate of all 6 measurements: 100 Hz

IMU - history

… torpedoes, rockets, airplanes, submarines - military weaponry.

• Nokia N95 – 2007 – one of the first smart phones
It has GPS, a built-in accelerometer, originally used for video stabilization and photo orientation.
• Latter Nokia has allowed software to use the data from inertial sensors and Pandora's box was opened and all the "evils" of the world were available for … about 2 billions users of smart phones today.

IMU - history

… earlier – few specialists designed the algorithms in secret laboratories on several places in the world, like Drapper Laboratory in MIT with unique multimillion equipment.

… now – hundreds of thousands programmers application hungry

Option panel of sensor stream application
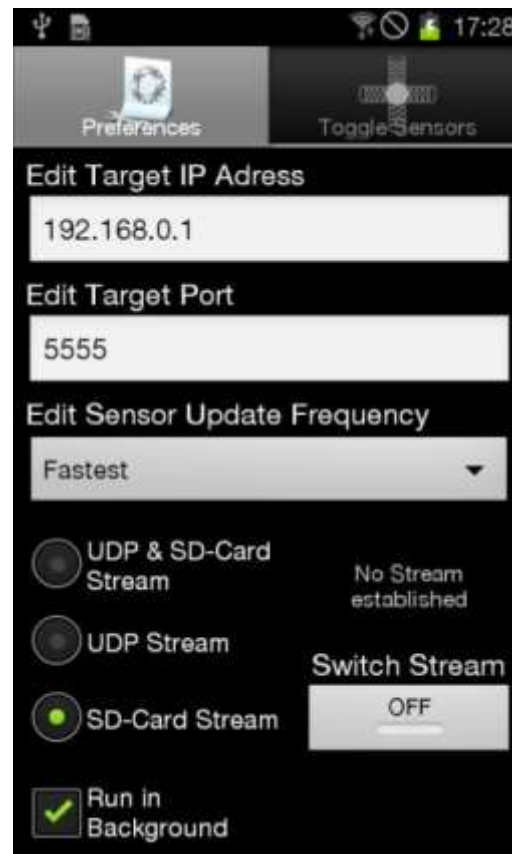
Sensor panel of sensor stream application

INS Functional Diagram
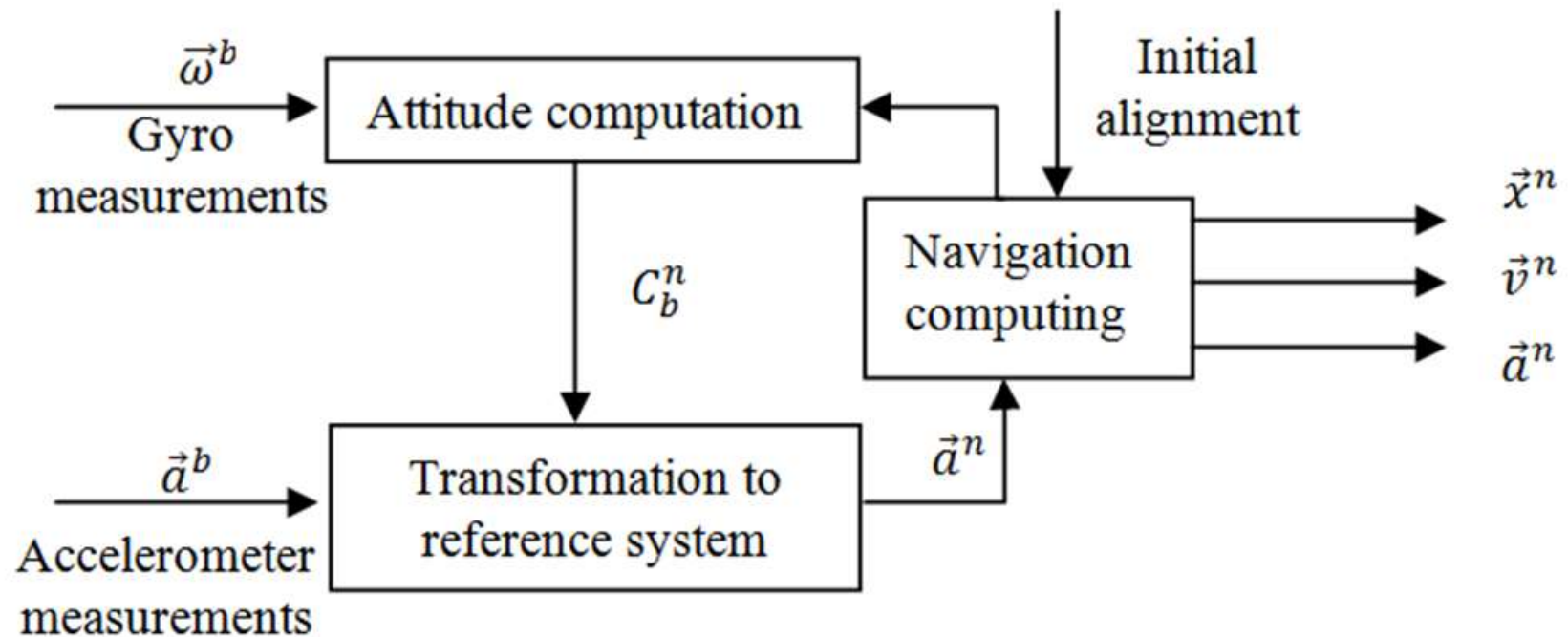
1) If the accelerometer measures acceleration with error, the corresponding distance error will be $\delta a \cdot t^2/2$, e.g. proportional to the square of the time.

2) If the gyro measures turn rate with error, after integration the error in attitude will be proportional to $\delta\varphi \cdot t$. But the attitude is applied to correct the orientation of acceleration vectors. The attitude error is spread over distance calculation and consequences are measured as $\delta\varphi \cdot t^3/6$.

Accuracy Analysis of IMU

Find a reference!

1) If you have a measuring equipment with at least one order of magnitude more accurate sensors.
2) If you have rotating device, which gives "exact" information about attitude and position
3) If you model sensors measurement
4) With real sensor data, but you plan the experiments with points with fixed position and attitude

Attitude computation

Naive integration approach for attitude calculation

$$
\begin{vmatrix} \varphi_k \\ \theta_k \\ \psi_k \end{vmatrix} = \begin{vmatrix} \varphi_0 \\ \theta_0 \\ \psi_0 \end{vmatrix} + \sum_k \begin{vmatrix} (\omega_x(k) + \omega_x(k-1))/2 \\ (\omega_y(k) + \omega_y(k-1))/2 \\ (\omega_z(k) + \omega_z(k-1))/2 \end{vmatrix} (t_k - t_{k-1})
$$

Attitude computation

Attitude calculation through Euler - Krylov algorithm

$$\dot{C}_b^n = C_b^n \Omega \times$$

$$\dot{\varphi} = \omega_x + tg\theta(sin\varphi * \omega_y + cos\varphi * \omega_z)$$

$$\dot{\theta} = cos\varphi * \omega_y - sin\varphi * \omega_z$$

$$\dot{\psi} = \frac{1}{cos\theta}\left(sin\varphi * \omega_y + cos\varphi * \omega_z\right)$$

Attitude computation

Using Poison differential equation for attitude calculation

$$\dot{C}_b^n = C_b^n \Omega \times$$

$$C_{k+1} = C_k \left(I + \frac{\sin \sigma_n}{\sigma_n} \sigma \times + \frac{1 - \cos \sigma_n}{\sigma_n^2} (\sigma \times)^2 \right)$$

Attitude computation
Quaternion approach

$$\dot{q} = 0.5 q \omega_q = 0.5 \begin{vmatrix} 0 & -\omega_x & -\omega_y & -\omega_z \\ \omega_x & 0 & \omega_z & -\omega_y \\ \omega_y & -\omega_z & 0 & \omega_x \\ \omega_z & \omega_y & -\omega_x & 0 \end{vmatrix} \begin{vmatrix} q_0 \\ q_1 \\ q_2 \\ q_3 \end{vmatrix}$$

$$q_{k+1} = q_k \left(A \otimes \sigma_q \right)$$

$$A = \begin{vmatrix} c \\ s \\ s \\ s \end{vmatrix}$$

$$c = 1 - \frac{(0.5\sigma)^2}{2!} + \frac{(0.5\sigma)^4}{4!} - \cdots$$

$$s = 0.5 \left(1 - \frac{(0.5\sigma)^2}{3!} + \frac{(0.5\sigma)^4}{5!} - \cdots \right)$$

The structure of IMU simulator
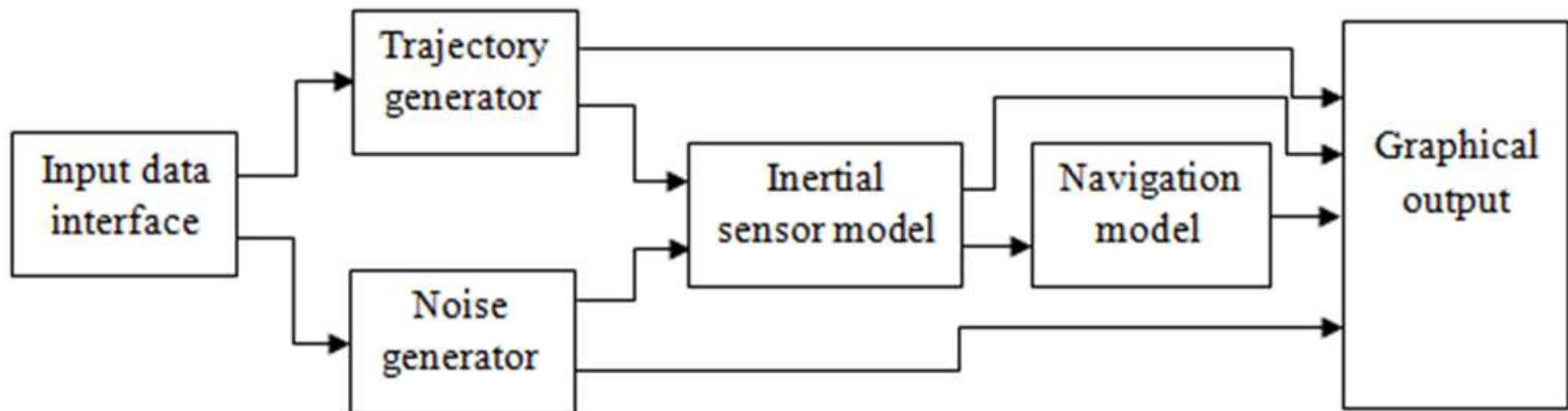
IMU simulator interface
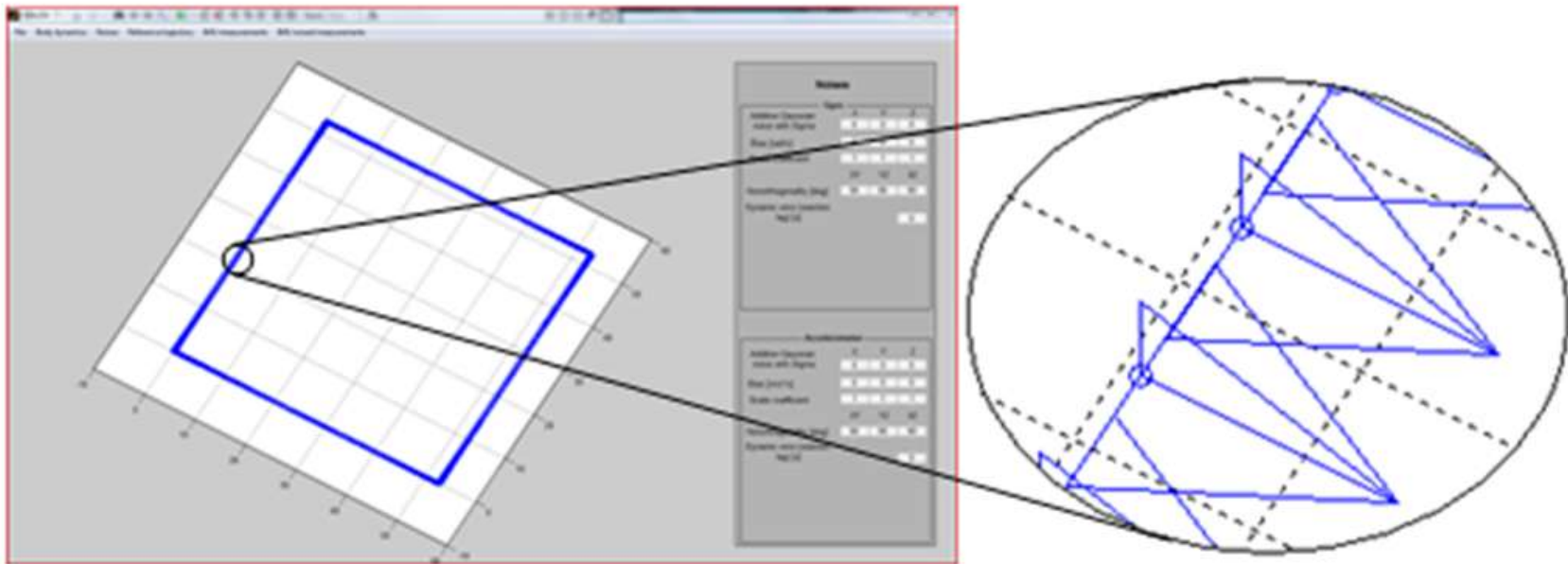
Modeled gyros data
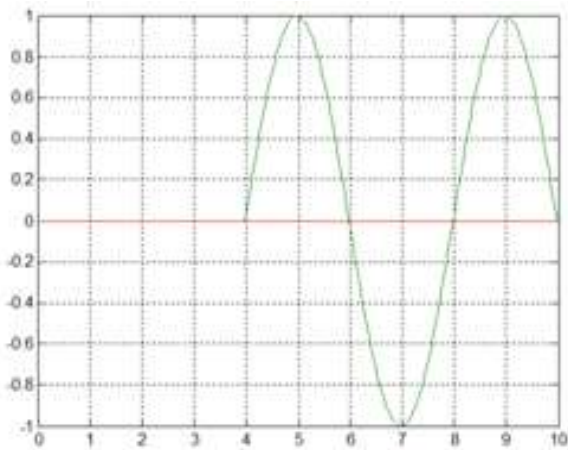
Fig. 2 Simple 1D rotation
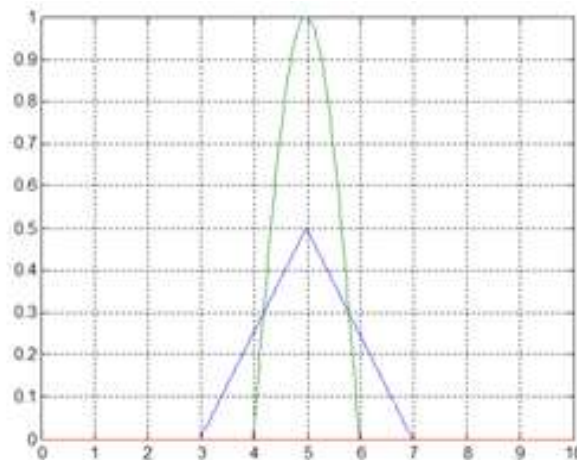
Fig. 3 2D overlapping rotations
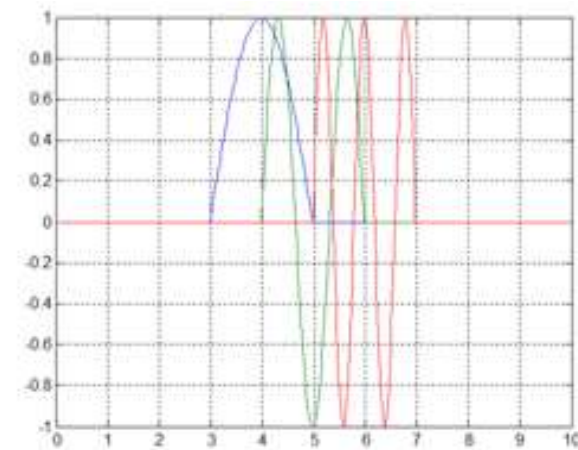
Fig. 4 3D overlapping rotation with different intensity

Modeled gyros data
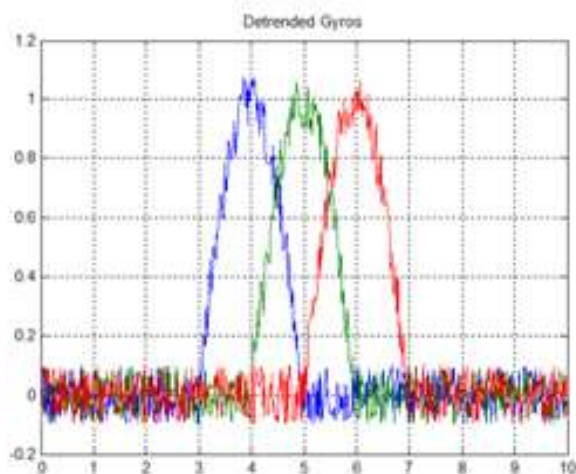
Fig. 5 Noised 3D
overlapping rotations
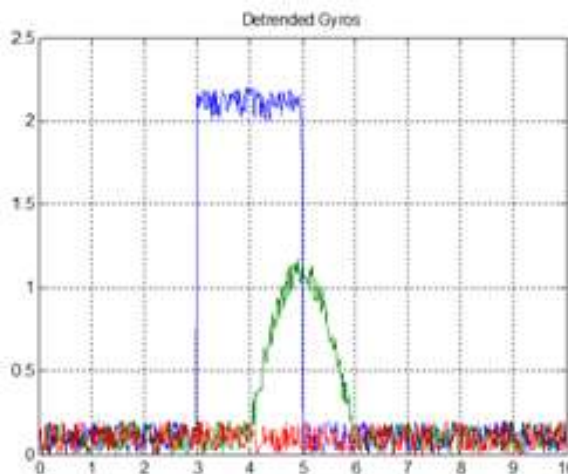
Fig. 6 Noised 2D
overlapping rotations
with bias
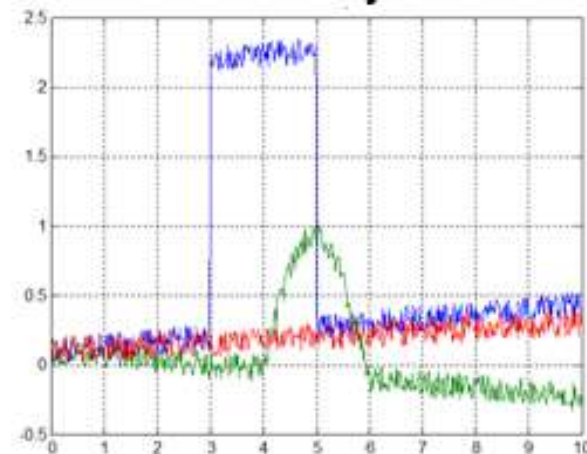
Fig. 7 Noised 2D
overlapping rotations
with different trends

Real gyros data
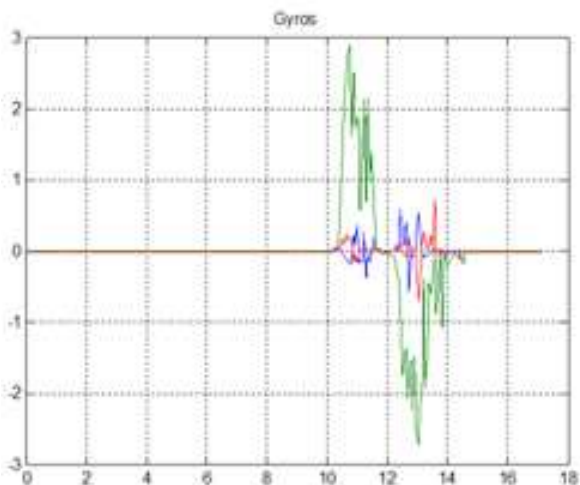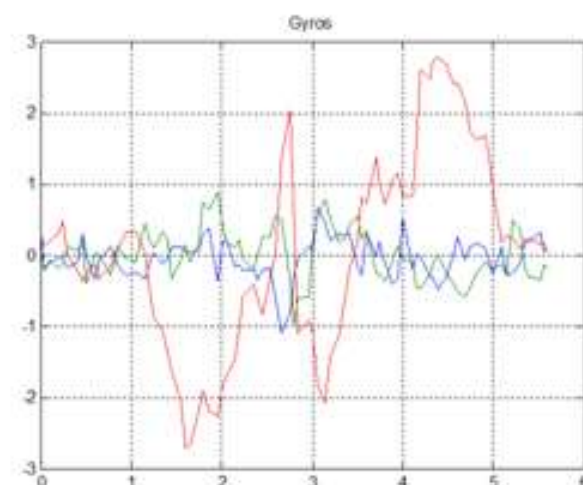

Fig. 8 1D real data
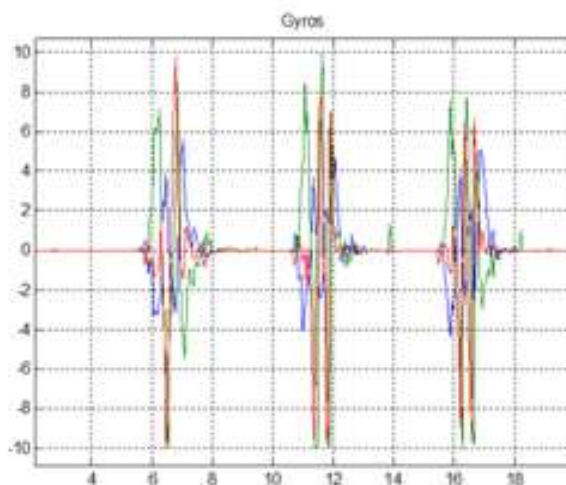
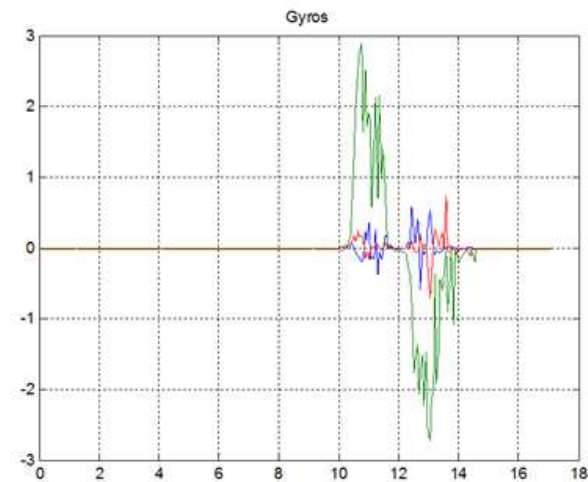Fig. 9 3D free rotations in cycle

Fig. 10 3D free rotations

Experimental results

Fig. 11 1D real data
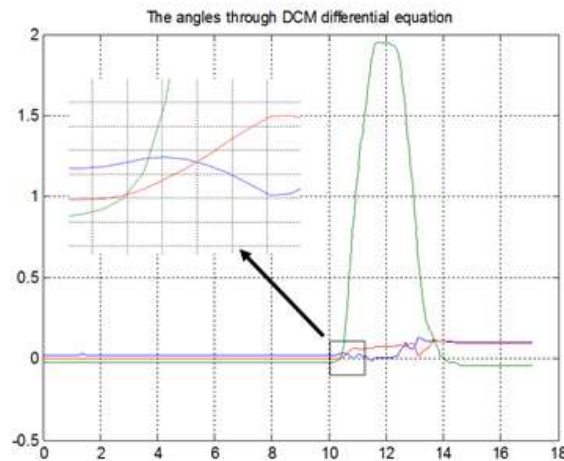
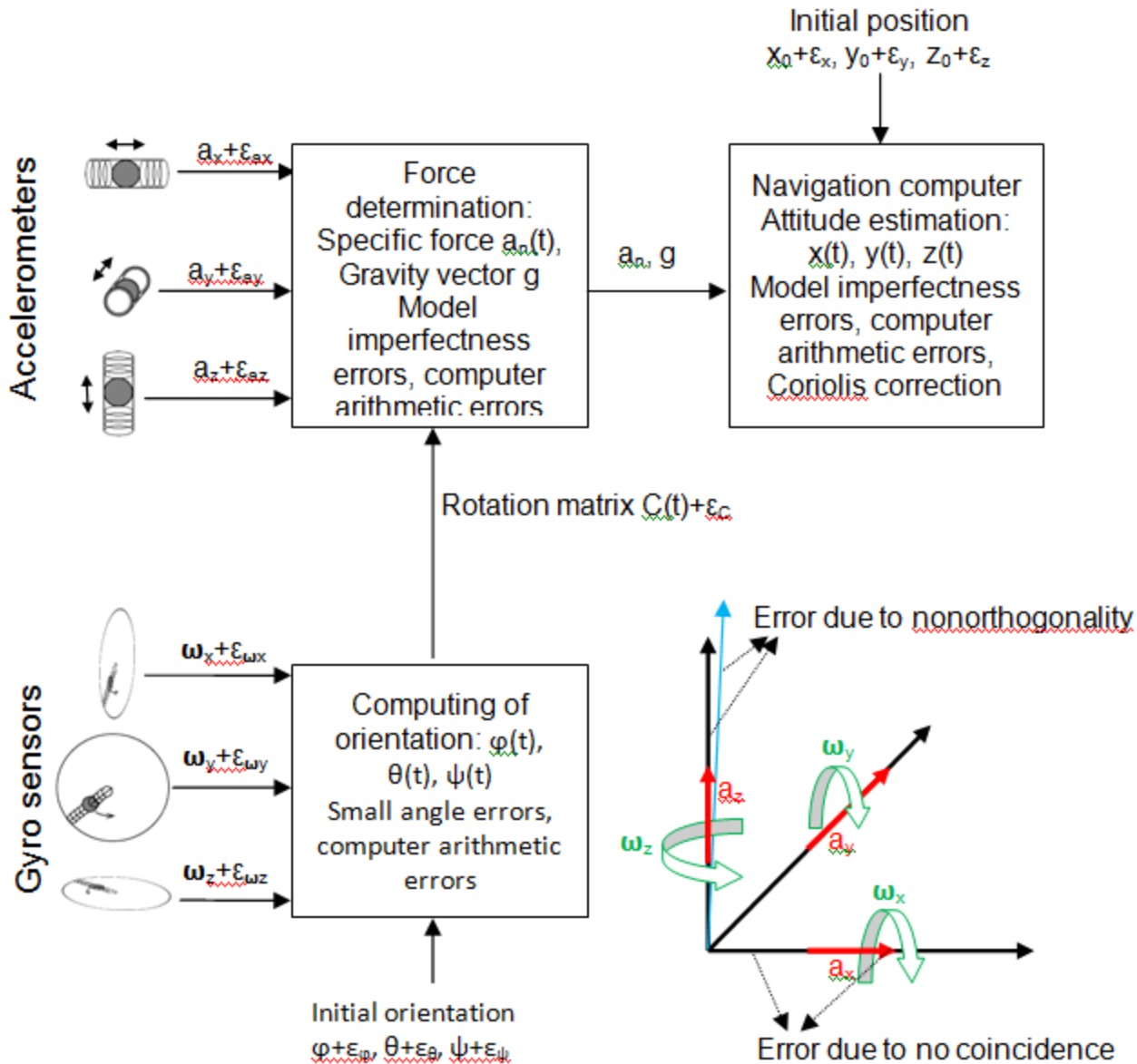Fig. 12 Correct integration of 1D real data
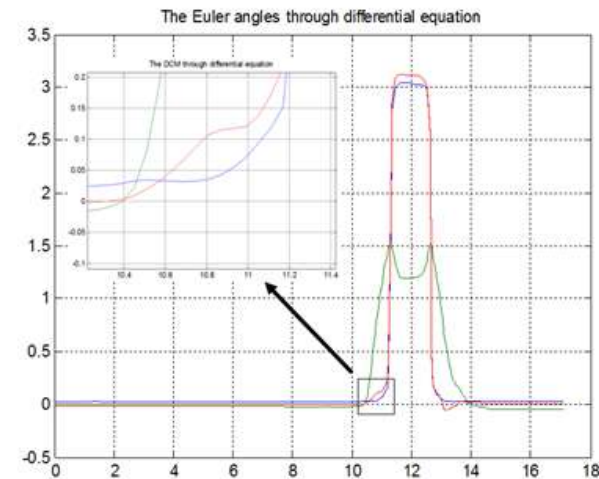
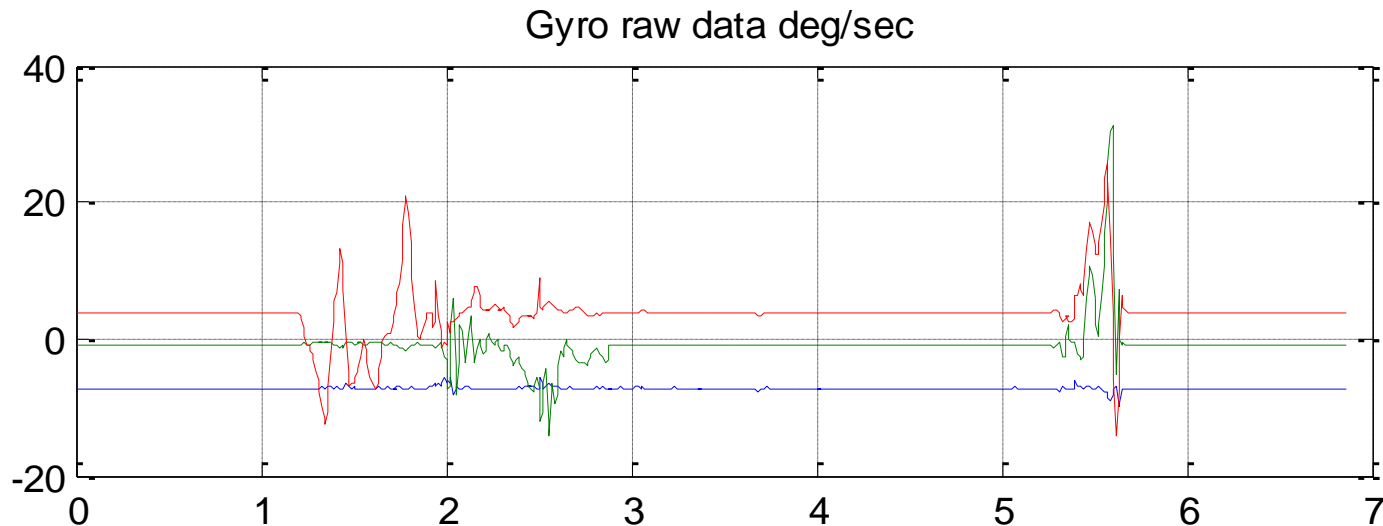Fig. 13 . Incorrect integration 1D real data

Gyro raw data deg/sec

Gyro shift correction deg/sec

Accelerometers raw data m/s^2

Accelerometers after calibration (scale and shift) m/s^2
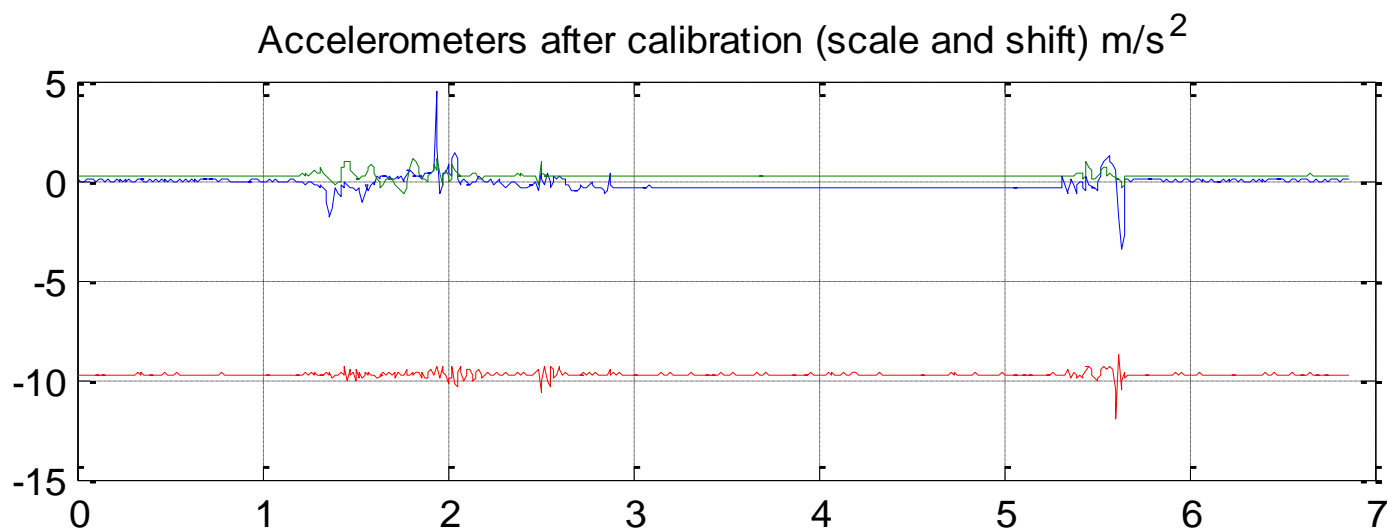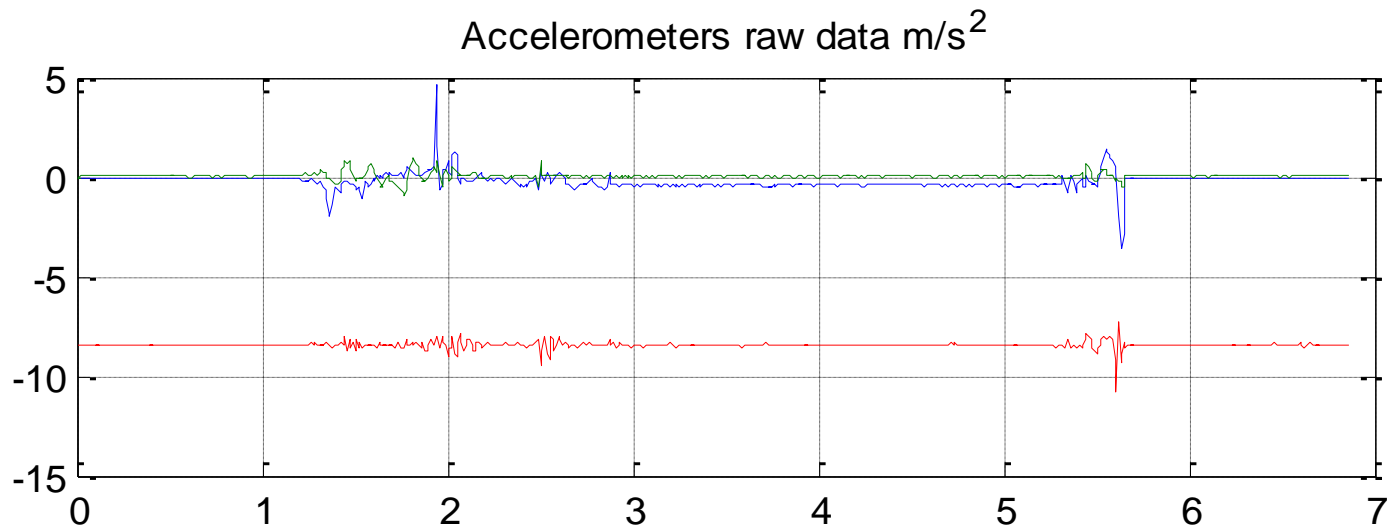
Calibration

a_x = (data_arr(6,:)-s1)/a1;

a_y = (data_arr(7,:)-s2)/a2;

a_z = (data_arr(8,:)-s3)/a3;

The shifts s1, s2, s3 and scaling coefficients a1,a2,a3 are estimated by optimization procedure with averaged data from several positions of the sensors

w_x_mean = mean(data_arr(2,1:70))
w_y_mean = mean(data_arr(3,1:70))
w_z_mean = mean(data_arr(4,1:70))
(no motion)

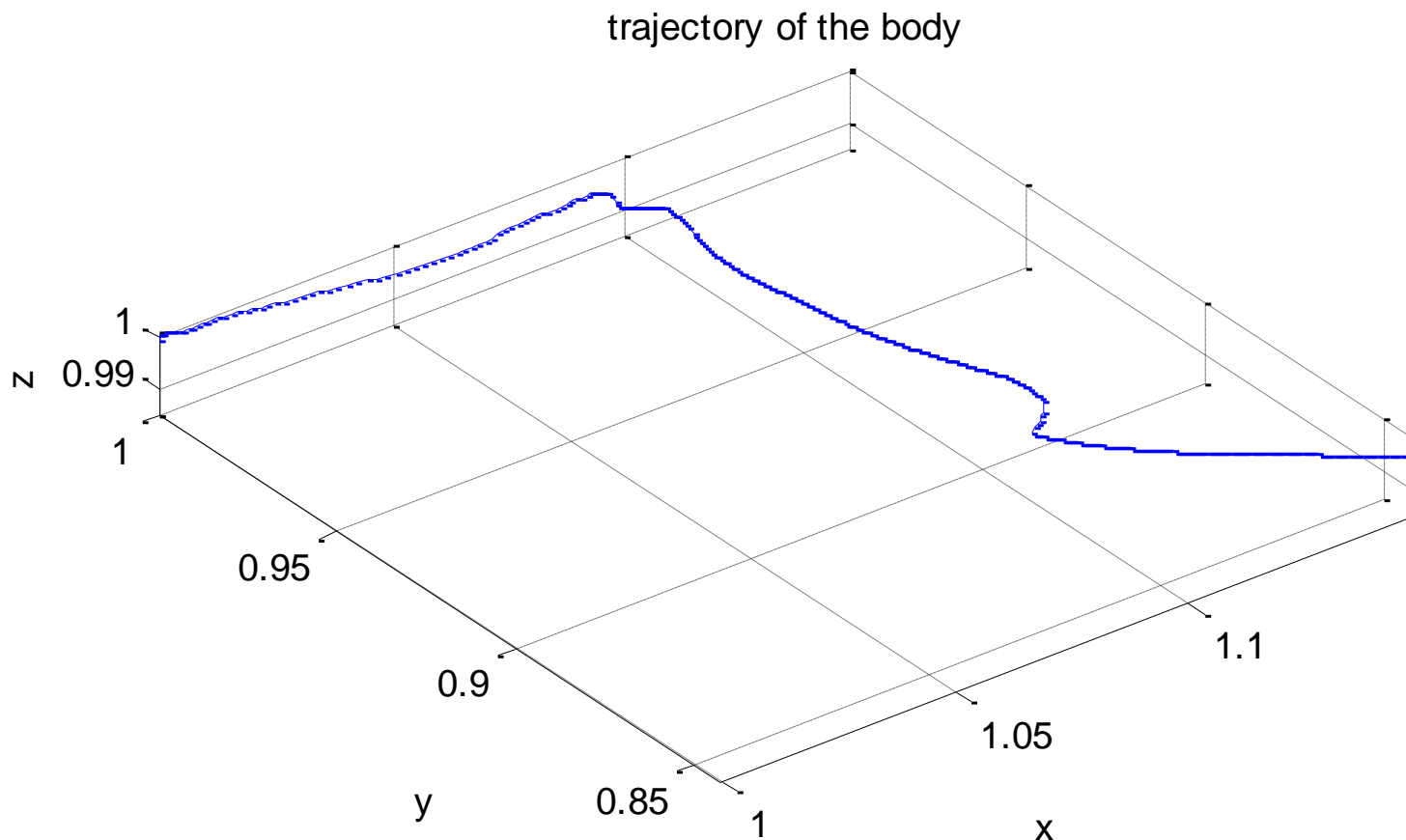**gyro_x = data_arr(2,:) - w_x_mean;**
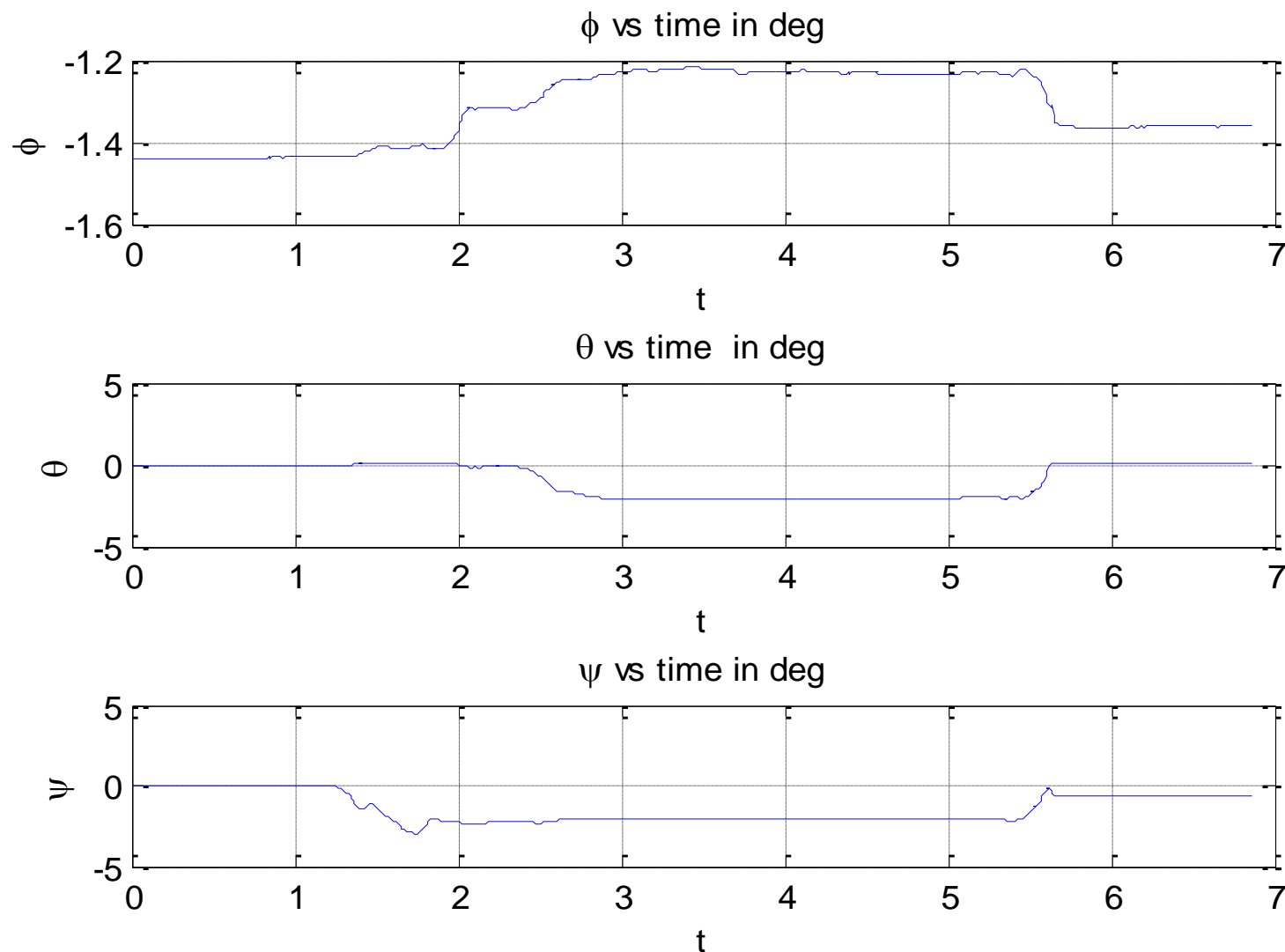**gyro_y = data_arr(3,:) - w_y_mean;**
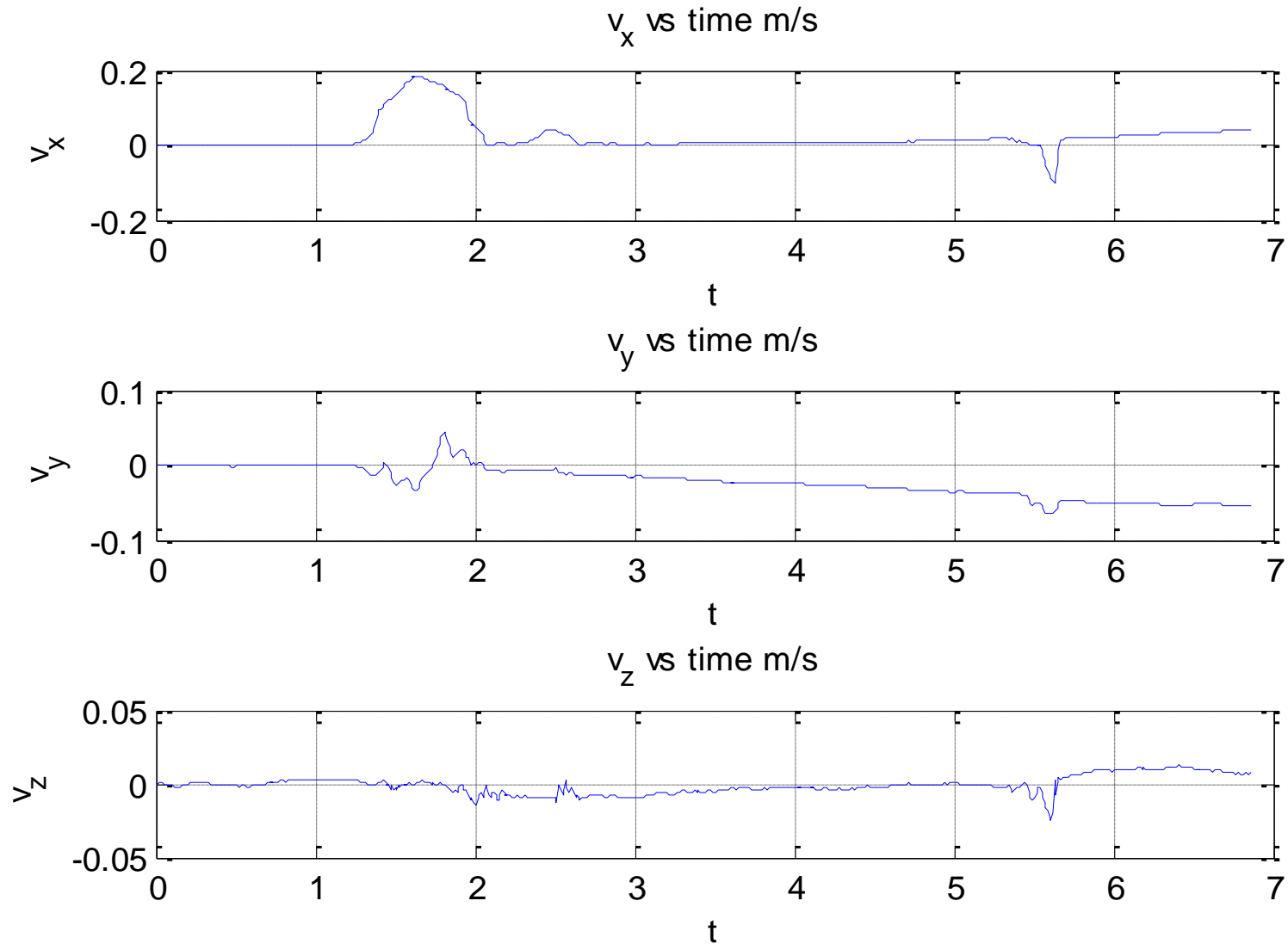**gyro_z = data_arr(4,:) - w_z_mean;**

Problem: nonconsistency:

s1 = -0.10364505886850;

s2 = -0.16361281148368;

s3 = 0.025479105123220;

a1 = 0.936997180377589;

a2 = 0.932347804777772;

a3 = 0.871907702114871;

g = 9.72112896

s1 = -0.05785805368620;

s2 = -0.14802497905120;

s3 = 0.025066179054880;

a1 = 0.930790162818945;

a2 = 0.927854935493497;

a3 = 0.874878855049987;

g = 9.687243

s1 = -0.083761479495474;

s2 = -0.2075773931498450;

s3 = 2.360384019177096;

a1 = 1.021526216348697;
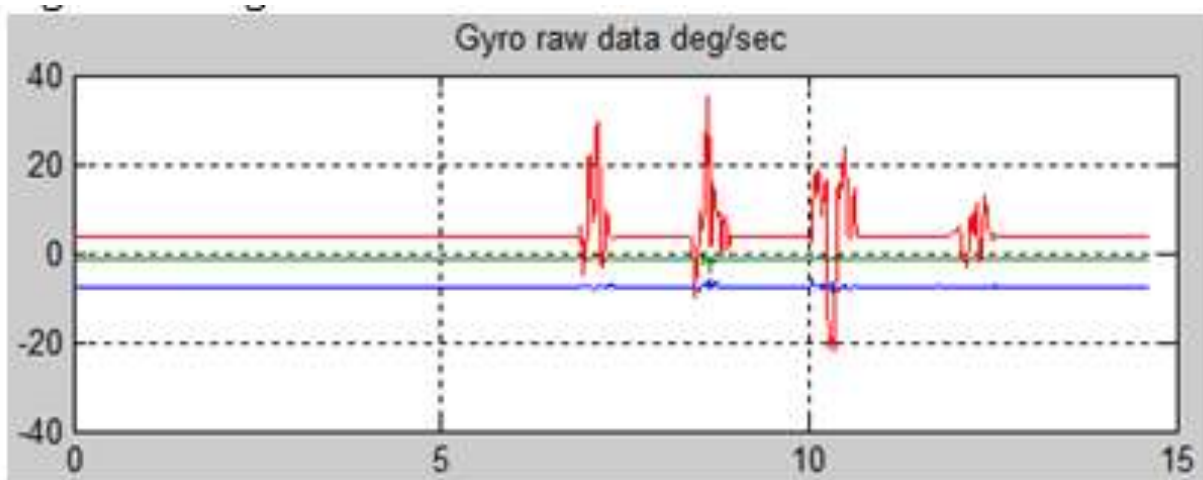
a2 = 1.009070389156962;

a3 = 1.109508357634151;

trajectory of the body

φ vs time in deg

θ vs time in deg

ψ vs time in deg

v_x vs time m/s

v_y vs time m/s

v_z vs time m/s

Figure 3. Gyro raw signals

Figure 4. Accelerometer raw signals

Trajectory of the body
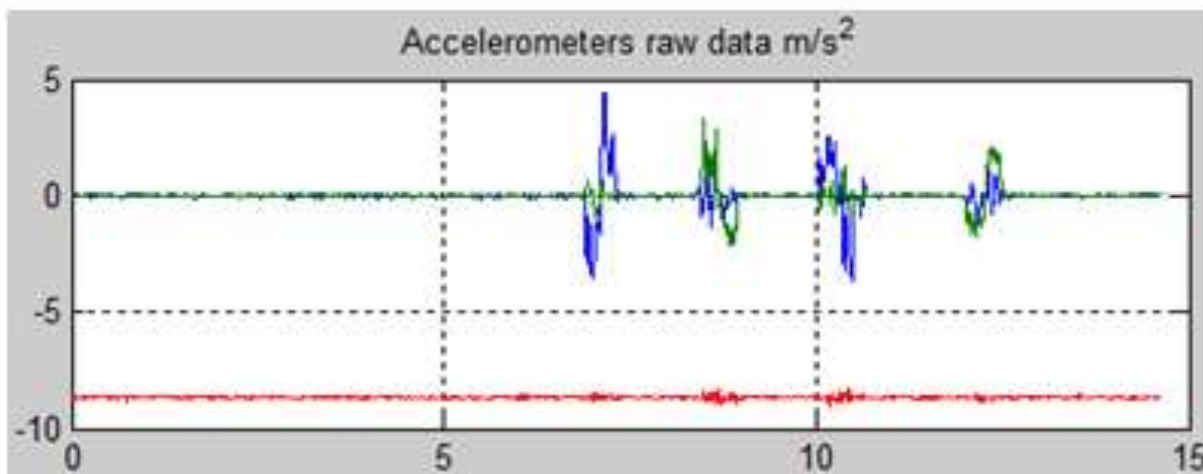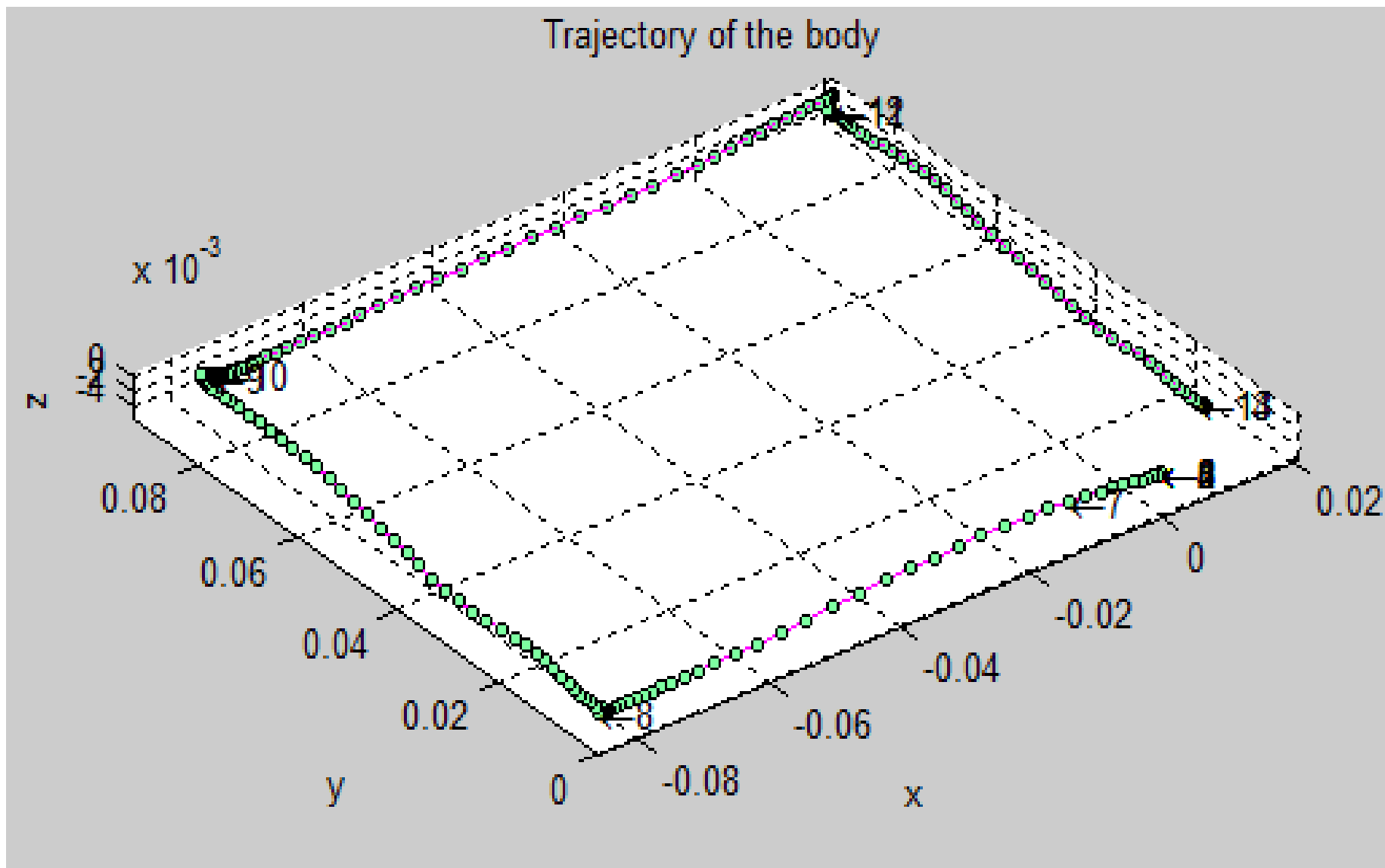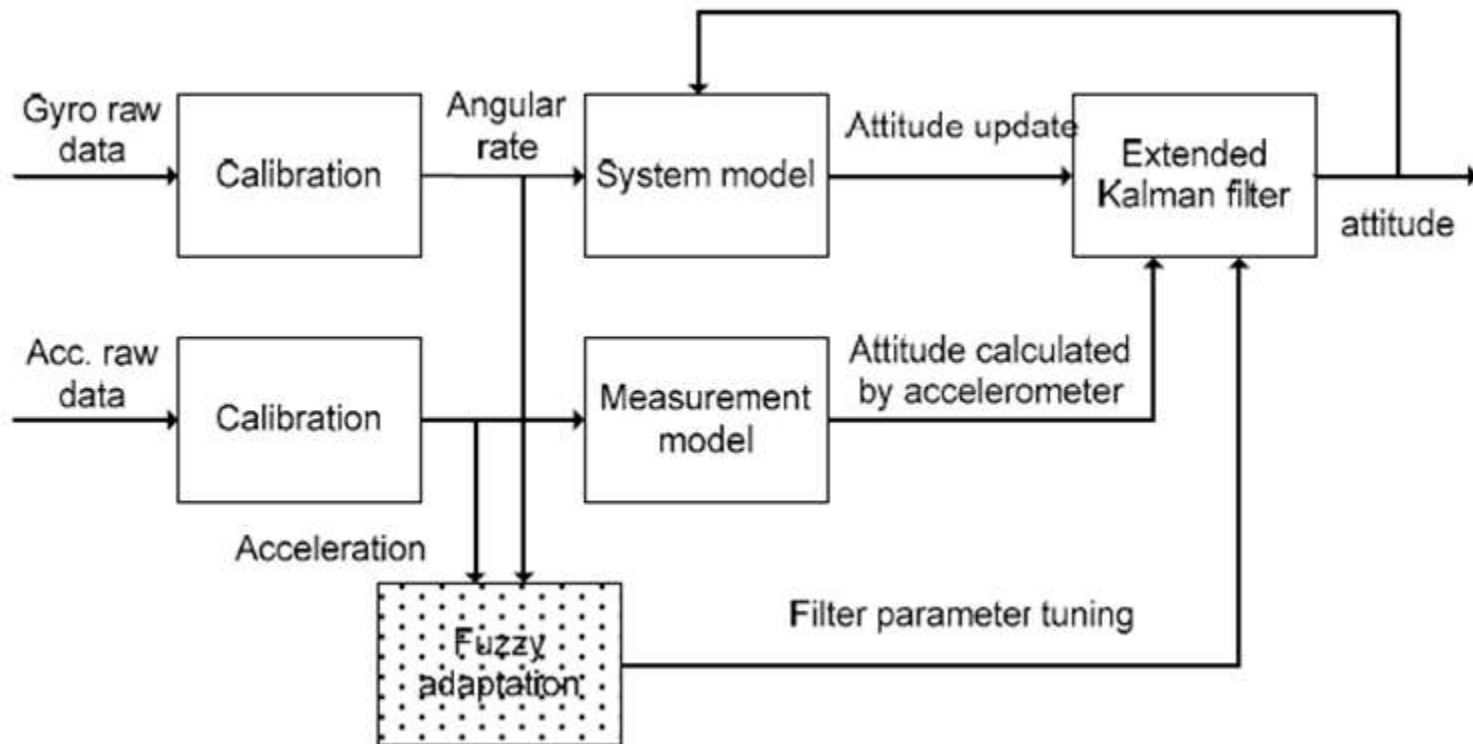
Initial angles determination: based on averaged data from non-moving accelerometers (no other information, we do not use compass)

Extended Kalman and fuzzy adaptation
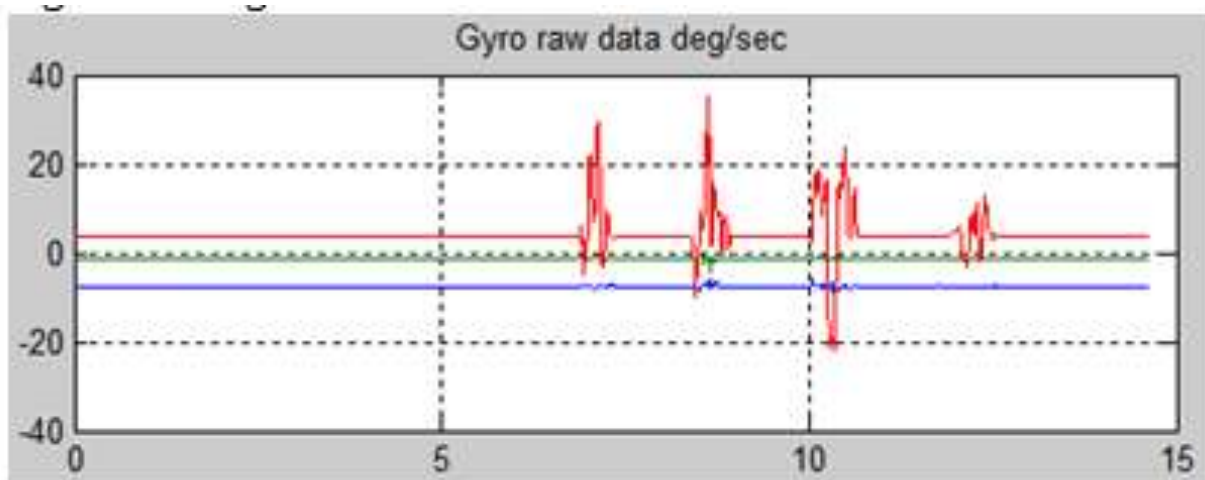
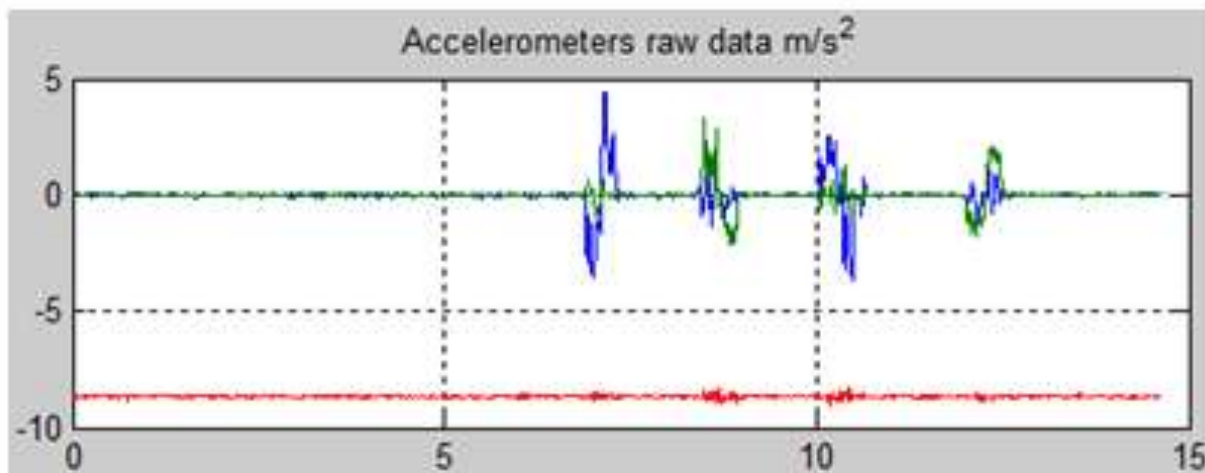# An approach for error reduction in IMU

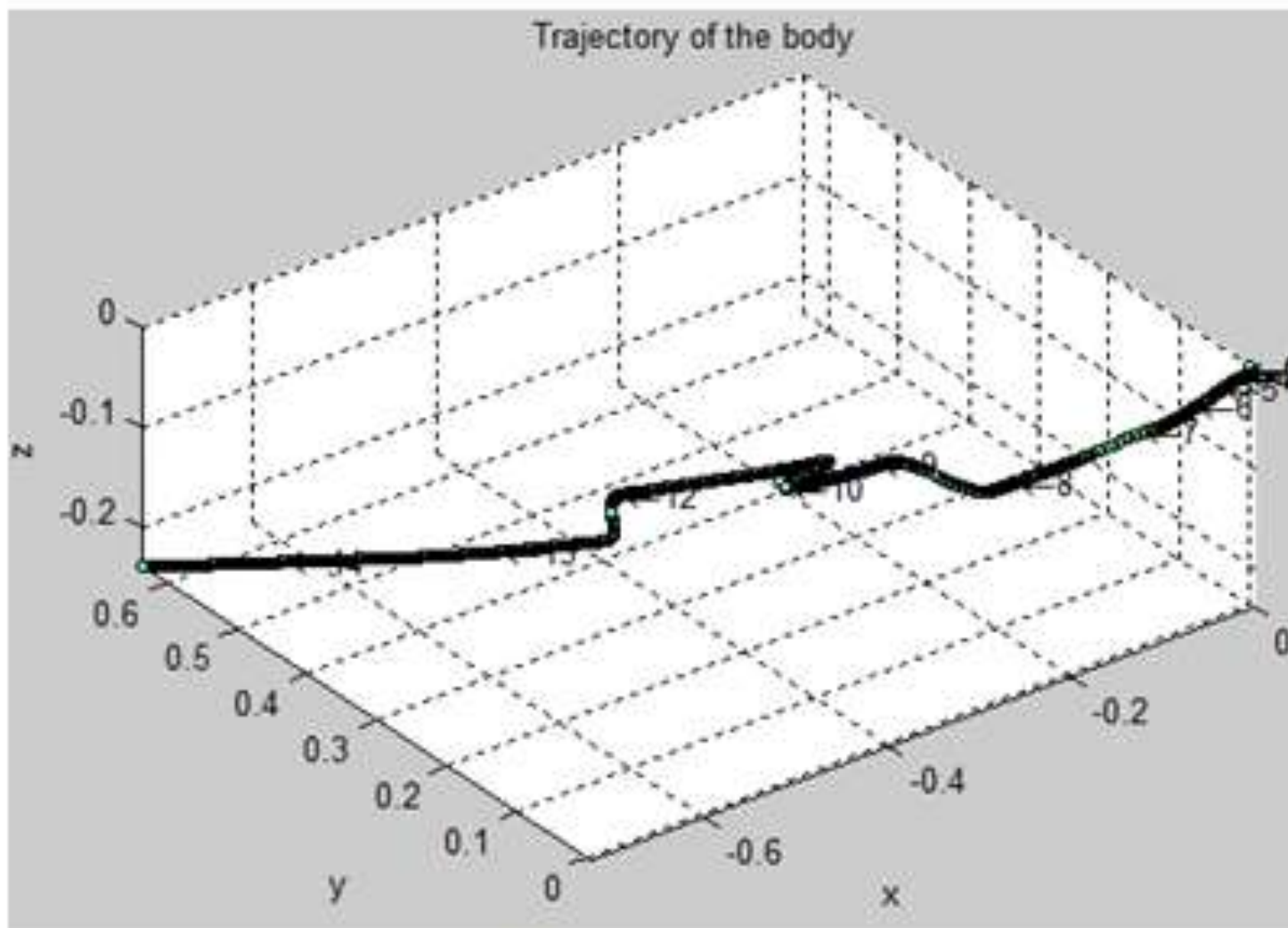Figure 3.   Gyro raw signals

Figure 4.   Accelerometer raw signals

Figure 2. The reconstracted platform trajectory without change detection

To minimize integration time we will discover motion of the platform and only when the motion is detected the integration process will be switched on. When there is no motion detected, the integration process will be stopped and the platform orientation and position will remain the same. This idea is not new one. For example, in the embedded software on newest MEMS an activity threshold is inserted for acceleration sensors. Only accelerations, exceeding threshold, switch on the flag "Activity". In spite of its simplicity the realization of this functionality gives the system engineers knowledge when to initialize the sensor or when to start recalibration procedure. In this work we develop this idea further. We realize more precise algorithm for activity detection, which is less susceptible from the sensor signal bias.

We are looking for a change of the mean of a sample with length equal to N by the following sufficient statistic [6]:

$$S_{j+1}^{j+N} = \frac{\mu_{k+1} - \mu_k}{\sigma^2} \sum_{i=j+1}^{j+N} \left(y_i - \mu_k - \frac{\mu_{k+1} - \mu_k}{2} \right), \text{ where}$$

$$\mu_k = \frac{1}{N} \sum_{i=NK+1}^{N(K+1)} y_i$$

The change is detected when the inequality is fulfilled:

$$\left| \mu_{k+1} - \mu_k \right| \geq m \frac{\sigma}{\sqrt{N}}$$

The tuning parameters of the procedure are m and N. The procedure is applied on the time-series from the all six inertial sensors – three gyros and three accelerometers. The output results are fused in a final time-series with two states only – "0" and "1". "Zero" means to stop integration of sensor output data and remains in the same state (the same position, velocity and acceleration) and preserve the same orientation of the platform in the space. When "One" appears for the first time the integration process is restarted and a new state vector and a new orientation of the platform are calculated.
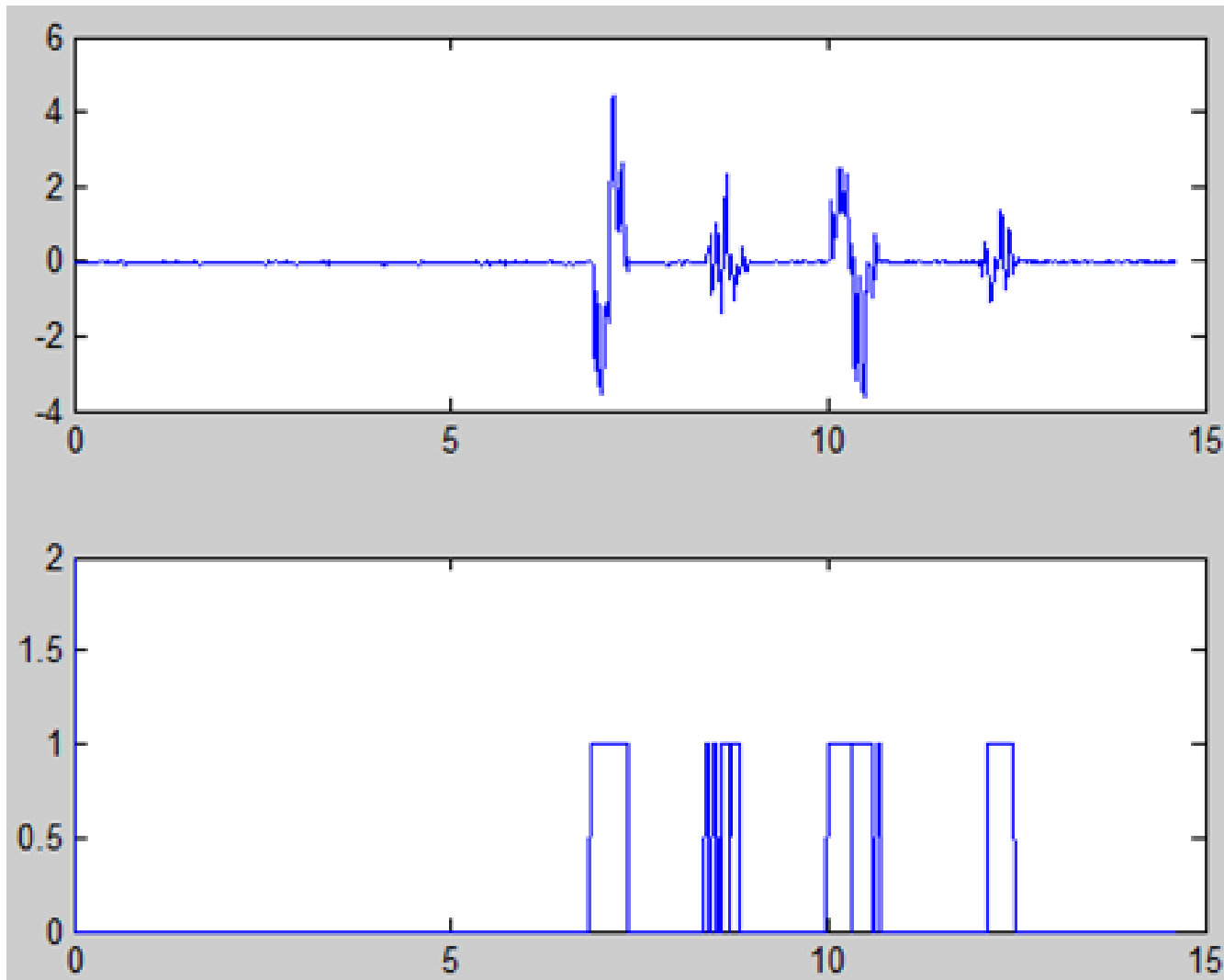
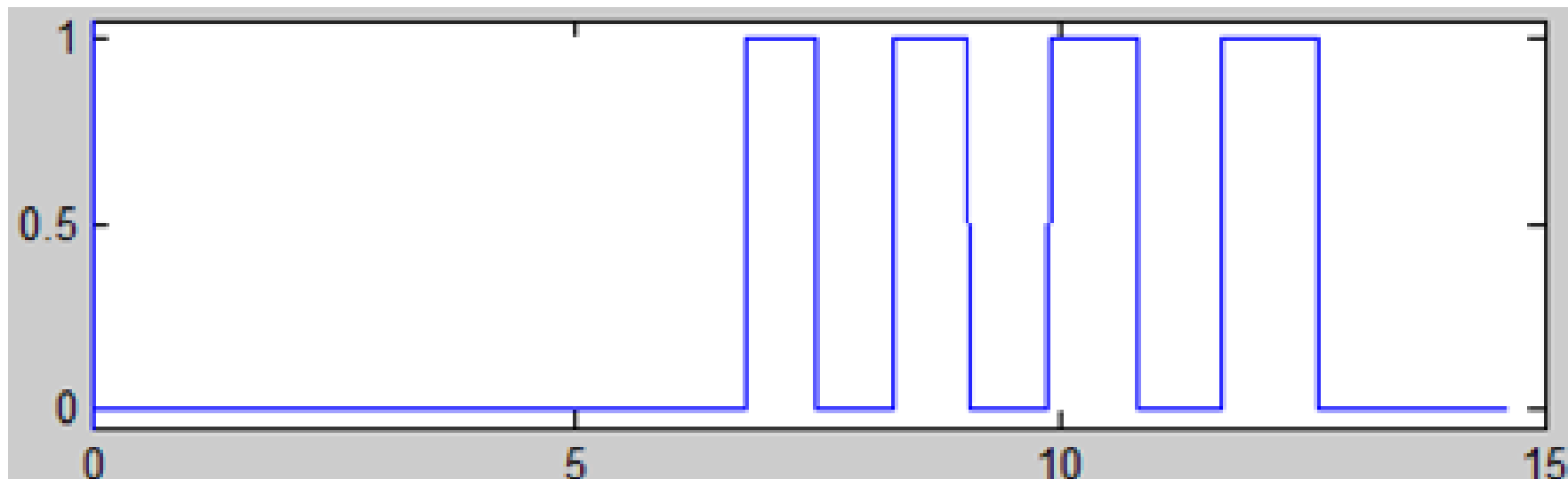Figure 5. Application of change detection algorithm on a raw signal

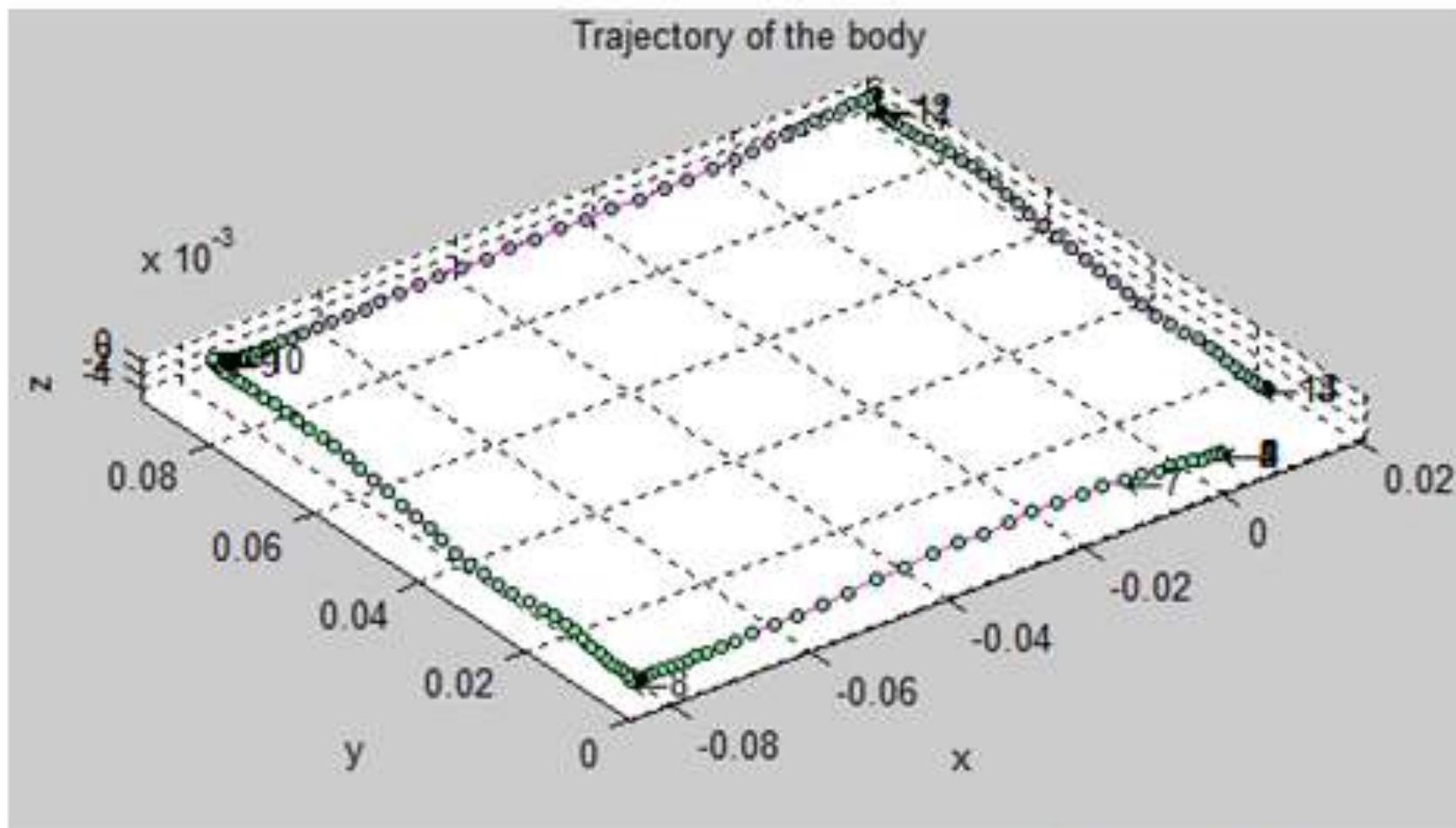Figure 6.   The fused result from change detection algorithm

Figure 7. The reconstracted platform trajectory with change detection

Now…

Open problems

1. Mathematical model

2. Calibration procedure

    - Initial alignment

    - real time (optimization procedure)

3. Kalman filter

4. Mathematical model for aided systems (integration with another sensor, fusion)

References

1. *http://www.vectornav.com/index.php?&id=76*
2. *David H. Titterton, John L. Weston Navigation Technology - 2nd Edition, The Institution of Electrical Engineers, 2004, ISBN 0 86341 358 7*
3. *Grewal, M.S., Weill L.R., Andrews A.P., Global Positioning Systems, Inertial Navigation, and Integration, John Wiley & Sons, 2001, ISBN 0-471-20071-9.*
4. *Oliver J. Woodman, An introduction to inertial navigation, Technical Report UCAM-CL-TR-696, ISSN 1476-2986, 2007.*

5. *http://www.sbir.gov/sbirsearch/detail/87111*
6. *http://www.americangnc.com/products/rtgis.htm*
7. *https://www.slideshare.net/gokullakshmanan/theory-of-gyrocompass-43492651*

Questions?